

A refined convergence estimate for a fourth order finite difference numerical scheme to the Cahn-Hilliard equation

Jing Guo* Cheng Wang† Yue Yan‡ Xingye Yue§

April 9, 2024

Abstract

In this article we present a refined convergence analysis for a second order accurate in time, fourth order finite difference numerical scheme for the 3-D Cahn-Hilliard equation, with an improved convergence constant. A modified backward differentiation formula temporal discretization is applied, and a Douglas-Dupont artificial regularization is included to ensure the energy stability. In fact, a standard application of discrete Gronwall inequality leads to a convergence constant dependent on the interface width parameter in an exponential singular form. We aim to obtain an improved estimate, with such a singular dependence only in a polynomial order. A uniform in time functional bounds of the numerical solution, including the higher order Sobolev norms, as well as the associated bounds for the first and second order temporal difference stencil, have to be carefully established. Certain recursive analysis has to be applied in the analysis for the BDF-style temporal stencil. As a result, we are able to apply a spectrum estimate for the linearized Cahn-Hilliard operator, and this technique leads to the refined error estimate. A three-dimensional numerical example of accuracy check is presented as well.

Key words. Cahn-Hilliard equation, long stencil fourth order finite difference approximation, BDF2 temporal discretization, linearized spectrum estimate, error analysis with an improved convergence constant

AMS Subject Classification 35K30, 35K55, 65M06, 65M12, 65T40

1 Introduction

In this article we consider the Cahn-Hilliard model. For any $\phi \in H^1(\Omega)$, with $\Omega \subset R^d$ ($d = 2$ or $d = 3$), the energy functional is given by (see [4] for a detailed derivation):

$$E(\phi) = \int_{\Omega} \left(\varepsilon^{-1} \left(\frac{1}{4} \phi^4 - \frac{1}{2} \phi^2 \right) + \frac{\varepsilon}{2} |\nabla \phi|^2 \right) d\mathbf{x}, \quad (1.1)$$

in which the parameter ε corresponds to the diffuse interface width. In turn, the Cahn-Hilliard equation becomes an H^{-1} conserved gradient flow of the energy functional (1.1):

$$\phi_t = \Delta \mu, \quad \mu := \delta_{\phi} E = \varepsilon^{-1} (\phi^3 - \phi) - \varepsilon \Delta \phi, \quad (1.2)$$

*School of Software Engineering, South China University of Technology, Guangzhou, Guangdong 510006, P. R. China (z7198185@gmail.com)

†Mathematics Department, The University of Massachusetts, North Dartmouth, MA 02747, USA (cwang1@umassd.edu)

‡School of Mathematics, Shanghai University of Finance and Economics, Shanghai 200433, P.R. China (corresponding author: yan.yue@mail.shufe.edu.cn)

§School of Mathematical Sciences, Soochow University, Suzhou, Jiangsu 215006, P. R. China (xyyue@suda.edu.cn)

where μ is the chemical potential. Periodic boundary conditions are imposed for both the phase field, ϕ , and the chemical potential, μ , as well as the higher order derivatives. Subsequently, the energy dissipation law follows from an inner product with (1.2) by μ : $E'(t) = -\int_{\Omega} |\nabla\mu|^2 d\mathbf{x} \leq 0$. Of course, since the dynamical equation is constructed as an H^{-1} gradient flow, the mass conservative identity is always valid: $\int_{\Omega} \partial_t \phi d\mathbf{x} = 0$.

Most existing numerical works for the Cahn-Hilliard equation have been focused on either the second order finite difference or linear/quadratic polynomial finite element spatial discretization. Meanwhile, a fourth order and even more accurate spatial approximation would be suitable to capture the more detailed structure with a reduced computational cost. Among the spatially higher order numerical algorithm for the Cahn-Hilliard equation, the spectral/pseudo-spectral approximation is worthy of investigation; see the related references [15, 16, 34, 36, 37, 38], etc. On the other hand, the spectral/pseudo-spectral differentiation corresponds to a global operator in space, and the associated numerical implementation requires an $O(N^d \ln N)$ float point calculations, instead of $O(N^d)$ scale for the finite difference ones. In contrast, a fourth order finite difference differentiation turns out to be a good choice to balance the high order spatial accuracy and the computational cost.

A second order accurate in time, fourth order long-stencil finite difference numerical scheme has been recently proposed and analyzed for the Cahn-Hilliard equation [12]. In the temporal approximation, a second order backward differentiation formula (BDF) stencil is applied, combined with a second order extrapolation formula applied to the concave diffusion term. Other than these standard discretization, a second order artificial Douglas-Dupont regularization term is included in the numerical algorithm to ensure the energy stability at a theoretical level, following similar ideas as [6, 7, 13, 19, 29, 35, 42, 50], etc. In addition, an optimal rate convergence analysis is derived for the numerical scheme, with second order temporal accuracy and fourth order spatial accuracy.

On the other hand, as always observed in the standard error estimate, an application of discrete Gronwall inequality leads to a convergence constant dependent on the final time T and on the interface parameter ε in a singular and exponential way. In more details, its dependence on T and ε is usually in a form of $\exp(C\varepsilon^{-m}T)$, with m an integer. To address this subtle issue, a few theoretical efforts have been reported to improve the convergence constant for the Allen-Cahn and Cahn-Hilliard equations, such as [22] for a first-order in time, fully discrete finite element scheme, [20, 21] for a first-order in time, discontinuous Galerkin scheme. In these theoretical works, the convergence constant is of order $O(e^{C_0 T} \varepsilon^{-m_0})$, for some positive integer m_0 and a constant C_0 independent on ε , instead of the singularly ε -dependent exponential growth. This improvement was based on a subtle spectrum analysis for the linearized Cahn-Hilliard operator (with certain given structure assumptions of the solution), provided in earlier PDE analysis literatures [1, 2, 8, 9, 10], etc.

Meanwhile, most existing works of improved convergence constant have been focused on the numerical scheme with first order accurate temporal discretization. A similar analysis has been performed for a semi-discrete, second order accurate in time numerical method in a more recent work [28], in which a modified Crank-Nicolson temporal approximation is taken, and the space is kept continuous in the analysis. In this article, we provide a refined convergence and error analysis for the second order accurate in time (modified BDF2 temporal discretization), fourth order long stencil difference numerical scheme for the 3-D Cahn-Hilliard equation, as proposed in [12].

The energy stability of the proposed numerical scheme has been proved in the existing work, which in turn gives a discrete H^1 bound of the numerical solution. Meanwhile, such a bound is not sufficient to derive a refined error estimate. To overcome the difficulty associated with the discrete Gronwall inequality, we have to analyze the numerical errors, which come from the nonlinear part, the concave linear part and the surface diffusion part, in a unified way. The spectrum estimate

for the linearized Cahn-Hilliard operator enables one to derive a refined estimate for the combined error. To achieve such a goal, a uniform in time (discrete) H^m (for $m \geq 2$) bound for the numerical solution is needed, in addition to the H^1 bound from the energy stability estimate. Such a bound could be theoretically accomplished by taking a discrete inner product with $(-\Delta_{h,(4)})^m \phi^{n+1}$ (with ϕ the numerical solution, $\Delta_{h,(4)}$, $\nabla_{h,(4)}$ the long stencil difference approximation), combined with repeatedly application of discrete Hölder inequality and Sobolev estimates. In particular, the associated estimates in the fourth order long-stencil difference approximation have to be carefully derived, with the help of the Fourier analysis and the eigenvalue analysis. Moreover, all these bounds are dependent on the initial H^m data, $\frac{1}{\varepsilon}$ (in a polynomial form), and independent on T . Since this bound is valid for any $m \geq 2$, a further observation indicates that $\|\phi^{n+1} - \phi^n\|_{H^k}$ (for an integer k) is always of order $O(\Delta t)$, and the constant is independent on T . In turn, a uniform in time $O(\Delta t)$ estimate for $\|\phi^{n+1} - \phi^n\|_{H^k}$ becomes available, and this bound turns out to be independent on the convergence analysis. More importantly, a difference analysis between $\phi^{n+1} - \phi^n$ and $\phi^n - \phi^{n-1}$ results in a uniform in time $O(\Delta t^2)$ estimate for $\|\phi^{n+1} - 2\phi^n + \phi^{n-1}\|_{H^k}$, with the constant dependent on $\frac{1}{\varepsilon}$ in a polynomial form, independent on T . Due to the extended structure of the BDF-style temporal stencil, in comparison with the Crank-Nicolson version [28], certain recursive analysis has to be applied in the analysis for the BDF2 temporal stencil.

In fact, these preliminary estimates play a crucial role in the refined error analysis. The numerical error evolutionary equation is evaluated at the time instant t^{n+1} , and its difference with the exact PDE solution is of order $O(\Delta t^2 + h^4)$, with the help of $\|\phi^{n+1} - 2\phi^n + \phi^{n-1}\|_{H^k}$ estimate, as well as the fourth order difference approximation analysis. In addition, to analyze the finite difference scheme over a uniform numerical grid, we estimate the difference between the discrete $\nabla_{h,(4)}$ norm of the numerical error function and the continuous H^1 norm of its continuous version, with the help of the discrete and continuous Fourier analysis. This Fourier analysis also enables us to perform an estimate for the difference between the discrete ℓ^2 inner product associated with the nonlinear term and its continuous version, and some aliasing error control techniques have to be applied [26]. As a result of these preliminary estimates, we are able to apply the spectrum analysis for the linearized Cahn-Hilliard operator [1, 2, 8], so that all the numerical error inner product terms, in the discrete H^{-1} space, are analyzed in a unified way. Such a unified error estimate leads to a coefficient of the numerical error, in the discrete H^{-1} norm, independent on ε . Consequently, we arrive at a discrete H^{-1} error estimate of order $O(\Delta t^2 + h^4)$, with the convergence constant in the form of $O(e^{C_0^* T} \varepsilon^{-m_0})$, with C_0^* independent on ε .

The outline of the paper is given as follows. In Section 2 we review the long stencil fourth order finite difference approximation, the proposed numerical scheme, and a few preliminary estimates. The main theoretical result is stated as well. The higher order H^m (for $m \geq 2$) numerical stability analysis is presented in Section 3. As a result, a uniform in time estimate for both $\|\phi^{n+1} - \phi^n\|_{H^k}$ and $\|\phi^{n+1} - 2\phi^n + \phi^{n-1}\|_{H^k}$ is derived as well. Subsequently, the primary convergence analysis is presented in Section 4. In more detail, a discrete H^{-1} error estimate of order $O(\Delta t^2 + h^4)$ is obtained, with the convergence constant dependent on $\frac{1}{\varepsilon}$ in a polynomial form. Moreover, a three-dimensional numerical example is presented in Section 5, to perform an accuracy check to validate the theoretical analysis. Some concluding remarks are made in Section 6. In the appendices we give the detailed proof of a few technical lemmas associated with the fourth order long stencil difference approximation, and provide a detailed analysis to estimate the difference between the discrete ℓ^2 inner product and its continuous version.

2 The numerical scheme and the main convergence result

2.1 The spatial discretization and the related notations

For simplicity of presentation, it is assumed that $\Omega = (0, L)^3$, and we denote $L = N \cdot h$, in which $h = \frac{L}{N}$ (N being a positive integer) stands for the mesh size. In turn, the following uniform, infinite grid with grid spacing $h > 0$: $E := \{x_i \mid i \in \mathbb{Z}\}$, with $x_i := (i - \frac{1}{2})h$, is introduced.

The derivation of long stencil fourth order finite difference formula is based on the Taylor expansion for the test function [23, 24, 32, 43]. For example, over a one-dimensional (1-D) uniform numerical grid, the fourth order approximations to the first and second order derivatives are formulated as

$$\mathcal{D}_{x,(4)}^1 f_i = \tilde{D}_x \left(1 - \frac{h^2}{6} D_x^2\right) f_i = \frac{f_{i-2} - 8f_{i-1} + 8f_{i+1} - f_{i+2}}{12h} = f'(x_i) + O(h^4), \quad (2.1)$$

$$\mathcal{D}_{x,(4)}^2 f_i = D_x^2 \left(1 - \frac{h^2}{12} D_x^2\right) f_i = \frac{-f_{i-2} + 16f_{i-1} - 30f_i + 16f_{i+1} - f_{i+2}}{12h^2} = f''(x_i) + O(h^4), \quad (2.2)$$

in which \tilde{D}_x and D_x^2 stand for the standard centered difference approximation to the first and second order derivatives, respectively. The long stencil fourth order difference method has been extensively applied to various physical models, such as incompressible Boussinesq equation [41, 48], geophysical fluid models [40, 45], the Maxwell equation [18], harmonic mapping flow [49], etc. Its advantage over the compact fourth order difference approximation [33, 39, 46] has also been described in [12].

Next, the following 3-D discrete periodic function space is taken into consideration:

$$\mathcal{V}_{\text{per}} := \{f : E \times E \times E \rightarrow \mathbb{R} \mid f_{i,j,k} = \nu_{i+\ell N, j+mN, k+nN}, \forall i, j, k, \ell, m, n \in \mathbb{Z}\}.$$

Meanwhile, the mean zero space is introduced to facilitate the later analysis:

$$\mathring{\mathcal{V}}_{\text{per}} := \left\{ f \in \mathcal{V}_{\text{per}} \mid \bar{f} := \frac{h^3}{|\Omega|} \sum_{i,j,k=1}^N f_{i,j,k} = 0 \right\}.$$

The fourth order 3-D discrete Laplacian, $\Delta_{h,(4)} : \mathcal{V}_{\text{per}} \rightarrow \mathcal{V}_{\text{per}}$, becomes

$$\Delta_{h,(4)} := \mathcal{D}_{x,(4)}^2 + \mathcal{D}_{y,(4)}^2 + \mathcal{D}_{z,(4)}^2.$$

Subsequently, the discrete inner product is defined as follows:

$$\langle f, g \rangle := h^3 \sum_{i,j,k=1}^N f_{i,j,k} g_{i,j,k}, \quad f, g \in \mathcal{V}_{\text{per}}.$$

For any $f \in \mathring{\mathcal{V}}_{\text{per}}$, there is a unique solution $\mathsf{T}_h[f] \in \mathring{\mathcal{V}}_{\text{per}}$ such that $-\Delta_{h,(4)} \mathsf{T}_h[f] = f$, and we denote $(-\Delta_{h,(4)})^{-1} f = \mathsf{T}_h[f]$. In turn, a discrete analog of the $\mathring{H}_{\text{per}}^{-1}$ inner product is introduced as

$$\langle f, g \rangle_{-1,h} := \langle f, (-\Delta_{h,(4)})^{-1} g \rangle = \langle (-\Delta_{h,(4)})^{-1} f, g \rangle, \quad f, g \in \mathring{\mathcal{V}}_{\text{per}}. \quad (2.3)$$

Of course, a discrete H^{-1} norm could be defined as $\|f\|_{-1,h}^2 = \langle f, f \rangle_{-1,h}$, for any $f \in \mathring{\mathcal{V}}_{\text{per}}$. If $f \in \mathcal{V}_{\text{per}}$, then $\|f\|_2^2 := \langle f, f \rangle$; $\|f\|_p^p := \langle |f|^p, 1 \rangle$ ($1 \leq p < \infty$), and $\|f\|_\infty := \max_{1 \leq i,j,k \leq N} |f_{i,j,k}|$.

In terms of the gradient inner product, the following notations are introduced:

$$[D_x f, D_x g]_x := \frac{1}{2} h^3 \sum_{i,j,k=1}^N ((D_x f)_{i+\frac{1}{2},j,k} (D_x g)_{i+\frac{1}{2},j,k} + (D_x f)_{i-\frac{1}{2},j,k} (D_x g)_{i-\frac{1}{2},j,k}), \quad (2.4)$$

$[\cdot, \cdot]_y$ and $[\cdot, \cdot]_z$ could be similarly defined,

$$\langle \nabla_h f, \nabla_h g \rangle := [D_x f, D_x g]_x + [D_y f, D_y g]_y + [D_z f, D_z g]_z, \quad \|\nabla_h f\|_2 := (\langle \nabla_h f, \nabla_h f \rangle)^{\frac{1}{2}}.$$

The following summation by parts formulas have been reported in [12]:

$$\langle f, -\Delta_{h,(4)} g \rangle = \langle -\Delta_{h,(4)} f, g \rangle = \langle \nabla_h f, \nabla_h g \rangle + \frac{h^2}{12} (\langle D_x^2 f, D_x^2 g \rangle + \langle D_y^2 f, D_y^2 g \rangle + \langle D_z^2 f, D_z^2 g \rangle), \quad (2.5)$$

$$\langle \mathbb{T}_h f, (-\Delta_{h,(4)}) g \rangle = \langle f, g \rangle, \quad \forall f, g \in \mathcal{V}_{\text{per}}^{\circ}. \quad (2.6)$$

As a result, the corresponding discrete gradient norm associated with the long stencil difference is given by

$$\|\nabla_{h,(4)} f\|_2^2 = \|\nabla_h f\|_2^2 + \frac{h^2}{12} (\|D_x^2 f\|_2^2 + \|D_y^2 f\|_2^2 + \|D_z^2 f\|_2^2). \quad (2.7)$$

Furthermore, the discrete $\|\cdot\|_{H_h^1}$ and $\|\cdot\|_{H_h^2}$ norms are needed in the later analysis:

$$\|f\|_{H_h^1}^2 := \|f\|_2^2 + \|\nabla_h f\|_2^2, \quad \|f\|_{H_h^2}^2 := \|f\|_{H_h^1}^2 + \|\Delta_h f\|_2^2. \quad (2.8)$$

Meanwhile, the discrete energy is defined as follows, for any $\phi \in \mathcal{V}_{\text{per}}$:

$$E_h(\phi) = \varepsilon^{-1} \left(\frac{1}{4} \|\phi\|_4^4 - \frac{1}{2} \|\phi\|_2^2 \right) + \frac{\varepsilon}{2} \|\nabla_{h,(4)} \phi\|_2^2. \quad (2.9)$$

The inequalities in the next lemma will play an important role in the energy stability and optimal rate convergence analysis; the proof has been provided in [12].

Lemma 2.1. [12] *We have*

$$\|\Delta_h f\|_2 \leq \|\Delta_{h,(4)} f\|_2 \leq \frac{4}{3} \|\Delta_h f\|_2, \quad \|\nabla_h f\|_2 \leq \|\nabla_{h,(4)} f\|_2 \leq \frac{2}{\sqrt{3}} \|\nabla_h f\|_2, \quad \forall f \in \mathcal{V}_{\text{per}}. \quad (2.10)$$

2.2 A few preliminary estimates

For simplicity of presentation, we assume $N_x = N_y = N_z = N = 2K + 1$ is odd. The general case can be analyzed in a similar manner.

For any grid function $f \in \mathcal{V}_{\text{per}}$, its discrete Fourier transformation is given by

$$f_{i,j,k} = \sum_{\ell,m,n=-K}^K \hat{f}_{\ell,m,n}^N e^{2\pi i(\ell x_i + m y_j + n z_k)/L}, \quad (2.11)$$

where $x_i = (i - \frac{1}{2})h$, $y_j = (j - \frac{1}{2})h$, $z_k = (k - \frac{1}{2})h$, and $\hat{f}_{\ell,m,n}^N$ are coefficients. Subsequently, we make its extension to a continuous function:

$$f_{\mathbf{F}}(x, y, z) = \sum_{\ell,m,n=-K}^K \hat{f}_{\ell,m,n}^N e^{2\pi i(\ell x + m y + n z)/L}. \quad (2.12)$$

The following preliminary estimates will play important role in the analysis in later sections. The proof of Lemma 2.2 has been provided in [27], while that of Lemmas 2.3 and 2.4 will be given in Appendix A, B. Also see the 1-D analysis in [44], with the centered difference approximation.

Lemma 2.2. [27] Suppose that $f, \Delta_h f \in \mathcal{V}_{\text{per}}$. Then we have

$$\|f\|_{H_h^2} \leq C \left(\|f\|_{H_h^1}^{\frac{2}{3}} \|\Delta_h^2 f\|_2^{\frac{1}{3}} + \|f\|_{H_h^1} \right), \quad (2.13)$$

$$\|f\|_{\infty} \leq C \left(\|f\|_{H_h^1}^{\frac{5}{6}} \|\Delta_h^2 f\|_2^{\frac{1}{6}} + \|f\|_{H_h^1} \right), \quad (2.14)$$

$$\|\nabla_h f\|_{\infty} \leq C \|f\|_{H_h^1}^{\frac{1}{2}} \|\Delta_h^2 f\|_2^{\frac{1}{2}}, \quad (2.15)$$

where $C > 0$ is a constant independent of h , and $\bar{\phi} := \frac{1}{|\Omega|} \langle \phi, 1 \rangle$ is the discrete average.

Lemma 2.3. Suppose that $f, \Delta_h^j f \in \mathcal{V}_{\text{per}}$. Then we have

$$D_{2j} \|\Delta^j \mathbf{f}_{\mathbf{F}}\| \leq \|\Delta_h^j f\|_2 \leq \|\Delta^j \mathbf{f}_{\mathbf{F}}\|, \quad \forall 0 \leq j \leq k, \quad (2.16)$$

$$D_{2j+1} \|\nabla \Delta^j \mathbf{f}_{\mathbf{F}}\| \leq \|\nabla_h \Delta_h^j f\|_2 \leq \|\nabla \Delta^j \mathbf{f}_{\mathbf{F}}\|, \quad \forall 0 \leq j \leq k, \quad (2.17)$$

$$\|\mathbf{f}_{\mathbf{F}}\|_{H^{-1}} \leq \|f\|_{-1,h} \leq D_{-1} \|\mathbf{f}_{\mathbf{F}}\|_{H^{-1}}, \quad \text{if } \bar{f} = 0, \quad (2.18)$$

$$\|\Delta_{h,(4)} f\|_2 \leq C_1 \|\Delta_{h,(4)}^2 f\|_2, \quad (2.19)$$

$$\|(\Delta_{h,(4)} f)_{\mathbf{F}}\|_{H^m} \leq \|\Delta f_{\mathbf{F}}\|_{H^m}, \quad \forall 0 \leq m \leq 2k - 1, \quad (2.20)$$

where $D_{2j}, D_{2j+1}, D_{-1} > 0$, $0 \leq j \leq k$, and $C_1 > 0$, are constants independent of h .

Lemma 2.4. Suppose that $f \in \mathcal{V}_{\text{per}}$. Then we have

$$0 \leq \|\nabla \mathbf{f}_{\mathbf{F}}\|^2 - \|\nabla_{h,(4)} f\|_2^2 \leq Ch^4 \|\mathbf{f}_{\mathbf{F}}\|_{H^3}^2, \quad (2.21)$$

where C is a constant independent of h .

Moreover, to analyze the finite difference scheme over a uniform grid, we have to estimate the discrete nonlinear inner product. To achieve this, some tools in the Fourier pseudo-spectral analysis have to be used. Denote \mathcal{B}^K as the space of trigonometric polynomials in x, y , and z of degree up to K (note that $N = 2K + 1$). For a continuous function \mathbf{f} with a Fourier series $\mathbf{f}(x, y, z) = \sum_{l,m,n=-\infty}^{\infty} \hat{\mathbf{f}}_{l,m,n} e^{2\pi i(lx+my+nz)/L}$, its projection onto the space \mathcal{B}^K is the following truncated series

$$\mathcal{P}_N \mathbf{f}(x, y, z) = \sum_{l,m,n=-K}^K \hat{\mathbf{f}}_{l,m,n} e^{2\pi i(lx+my+nz)/L}. \quad (2.22)$$

On the other hand, for \mathbf{f} which may not be in \mathcal{B}^K , an interpolation operator is defined as

$$\mathcal{I}_N \mathbf{f}(x, y, z) = f_{\mathbf{F}}(x, y, z), \quad (2.23)$$

in which f is the discrete grid function created by the interpolation of \mathbf{f} : $f_{i,j,k} = \mathbf{f}(x_i, y_j, z_k)$, $0 \leq i, j, k \leq N - 1$. Clearly $\mathcal{I}_N \mathbf{f} \neq \mathbf{f}$, due to the appearance of an aliasing error; their Fourier coefficients are different, unless $\mathbf{f} \in \mathcal{B}^K$. See the related references [3, 25, 30, 47], etc. On the other hand, a standard approximation analysis shows that, as long as \mathbf{f} and all derivatives (up to m -th order) are continuous and periodic on Ω , the convergence of the derivatives of the projection and interpolation is given by

$$\|\mathbf{f}(x, y, z) - \mathcal{P}_N \mathbf{f}(x, y, z)\|_{H^k} \leq Ch^{m-k} \|\mathbf{f}\|_{H^m}, \quad 0 \leq k \leq m, \quad (2.24)$$

$$\|\mathbf{f}(x, y, z) - \mathcal{I}_N \mathbf{f}(x, y, z)\|_{H^k} \leq Ch^{m-k} \|\mathbf{f}\|_{H^m}, \quad 0 \leq k \leq m, m > \frac{d}{2}. \quad (2.25)$$

See the related discussion of approximation theory [5]; a similar aliasing error control result is also available in a more recent work [26].

We denote $\Phi(\mathbf{x}, t)$ as the exact solution of the CH equation (1.2), with a smooth initial data. In turn, the Fourier projection is taken as $\Phi_N(\mathbf{x}, t) = \mathcal{P}_N \Phi(\mathbf{x}, t)$. Of course, the following projection approximation is valid, for any $0 \leq k \leq m$:

$$\|\Phi_N\|_{L^\infty(0,T;H^k)} \leq \|\Phi\|_{L^\infty(0,T;H^k)}, \quad \|\Phi_N - \Phi\|_{L^\infty(0,T;H^k)} \leq Ch^{m-k} \|\Phi\|_{L^\infty(0,T;H^m)}, \quad (2.26)$$

$$\|\partial_t^\ell \Phi_N\|_{L^\infty(0,T;H^k)} \leq \left\| \partial_t^\ell \Phi \right\|_{L^\infty(0,T;H^k)}, \quad \forall \ell \geq 1, \quad (2.27)$$

$$\|\partial_t^\ell (\Phi_N - \Phi)\|_{L^\infty(0,T;H^k)} \leq Ch^{m-k} \|\partial_t^\ell \Phi\|_{L^\infty(0,T;H^m)}, \quad \forall \ell \geq 1. \quad (2.28)$$

The following result plays a very important role in the nonlinear inner product analysis; its proof will be given in Appendix C. The proof in the 1-D version has been provided in [44].

Lemma 2.5. *Suppose \mathbf{f} and \mathbf{g} are continuous and periodic functions, and their discrete interpolation grid versions are given by f, g , respectively.*

(1) *If $\mathbf{f}, \mathbf{g} \in \mathcal{B}^K$, we have*

$$\langle f, g \rangle = (\mathbf{f}, \mathbf{g}). \quad (2.29)$$

(2) *In general, the following estimate is valid:*

$$|\langle f, g \rangle - (\mathbf{f}, \mathbf{g})| \leq Ch^8 (\|\mathbf{f}\|_{H^8} \cdot \|\mathbf{g}\|_{H^2} + \|\mathbf{f}\|_{H^2} \cdot \|\mathbf{g}\|_{H^8}), \quad (2.30)$$

in which C is a constant independent of h .

2.3 The fully discrete numerical scheme and the energy stability

A modified BDF2 temporal discretization is applied to the Cahn-Hilliard equation, combined with long stencil fourth order difference spatial approximation in space:

$$\begin{aligned} \frac{\frac{3}{2}\phi^{n+1} - 2\phi^n + \frac{1}{2}\phi^{n-1}}{\Delta t} &= \Delta_{h,(4)}\mu^{n+1}, \\ \mu^{n+1} &= \varepsilon^{-1}((\phi^{n+1})^3 - 2\phi^n + \phi^{n-1}) - \varepsilon\Delta_{h,(4)}\phi^{n+1} \\ &\quad - A\varepsilon^{-2}\Delta t\Delta_{h,(4)}(\phi^{n+1} - \phi^n). \end{aligned} \quad (2.31)$$

In terms of the convergence analysis, we compare the numerical solution with the projection solution Φ_N , instead of the exact solution Φ , to simplify the discrete H^{-1} error estimate. By Φ_N^m we denote $\Phi_N(\cdot, t^m)$, with $t^m = m \cdot \Delta t$. Since $\Phi_N \in \mathcal{B}^K$, the mass conservative property is available at the discrete level:

$$\overline{\Phi_N^m} = \frac{1}{|\Omega|} \int_{\Omega} \Phi_N(\cdot, t_m) d\mathbf{x} = \frac{1}{|\Omega|} \int_{\Omega} \Phi_N(\cdot, t_{m-1}) d\mathbf{x} = \overline{\Phi_N^{m-1}}, \quad \forall m \in \mathbb{N}. \quad (2.32)$$

On the other hand, the solution of the proposed scheme (2.31) is also mass conservative at the discrete level:

$$\overline{\phi^m} = \overline{\phi^{m-1}}, \quad \forall m \in \mathbb{N}. \quad (2.33)$$

Meanwhile, we use the mass conservative projection for the initial data:

$$\phi_{i,j,k}^0 = \Phi_N(x_i, y_j, z_k, t = 0). \quad (2.34)$$

The error grid function is defined as

$$e^k := \Phi_N^k - \phi^k, \quad \forall k \in \mathbb{N}. \quad (2.35)$$

Therefore, it follows that $\overline{e^k} = 0$, for any $k \in \mathbb{N}$, so that the discrete norm $\|\cdot\|_{-1,h}$ is well defined for the error grid function.

Since the proposed numerical method (2.31) is a two-step algorithm, a “ghost” point extrapolation for ϕ^{-1} is needed to preserve the second order accuracy in time. As outlined above, the initial value is taken as $\phi_{i,j,k}^0 = \Phi_N(x_i, y_j, z_k, t = 0)$. At the “ghost” time instant t^{-1} , the following approximation is taken:

$$\phi^{-1} = \phi^0 - \Delta t \Delta_{h,(4)} \mu_h^0, \quad \text{with } \mu_h^0 := \varepsilon^{-1}((\phi^0)^3 - \phi^0) - \varepsilon \Delta_{h,(4)} \phi^0. \quad (2.36)$$

Of course, the Taylor expansion implies an $O(\Delta t^2 + h^4)$ accuracy for this approximation:

$$\|\phi^{-1} - \Phi^{-1}\|_2 \leq C(\Delta t^2 + h^4). \quad (2.37)$$

The unique solvability, energy stability, as well as a discrete H^1 stability of the numerical solution, have been proved in [12].

Theorem 2.6. [12] *Given $\phi^k, \phi^{k-1} \in \mathcal{V}_{\text{per}}$, with $\overline{\phi^k} = \overline{\phi^{k-1}}$, there exists a unique solution $\phi^{k+1} \in \mathcal{V}_{\text{per}}$ for the numerical scheme (2.31). And also, this scheme is mass conservative, i.e., $\overline{\phi^k} \equiv \overline{\phi^0} := \beta_0$, for any $k \geq 0$. For $k \geq 1$, we introduce*

$$\mathcal{E}_h(\phi^{k+1}, \phi^k) := E_h(\phi^{k+1}) + \frac{1}{4\Delta t} \|\phi^{k+1} - \phi^k\|_{-1,h}^2 + \frac{1}{2\varepsilon} \|\phi^{k+1} - \phi^k\|_2^2. \quad (2.38)$$

For $A \geq \frac{1}{16}$, a modified energy-decay property is available for the numerical scheme (2.31):

$$\mathcal{E}_h(\phi^{k+1}, \phi^k) \leq \mathcal{E}_h(\phi^k, \phi^{k-1}). \quad (2.39)$$

Furthermore, suppose that the initial data are sufficiently regular so that

$$E_h(\phi^0) + \frac{\Delta t}{4} \|\nabla_{h,(4)} \mu_h^0\|_2^2 + \frac{\Delta t^2}{2} \|\Delta_{h,(4)} \mu_h^0\|_2^2 \leq \tilde{C}_0,$$

for some \tilde{C}_0 that is independent of h , and $A \geq \frac{1}{16}$. Then we have the following uniform (in time) H_h^1 bound for the numerical solution:

$$\|\phi^m\|_{H_h^1} \leq \tilde{C}_{1,\varepsilon} = O(\varepsilon^{-1}), \quad \forall m \geq 1, \quad (2.40)$$

in which $\tilde{C}_{1,\varepsilon}$ only depends on Ω , ε and \tilde{C}_0 , independent on h , Δt and final time. In more detail, its dependence on ε^{-1} is in a polynomial form, namely $O(\varepsilon^{-1})$.

As a consequence of Theorem 2.6 and the estimate (2.17), combined with the definition $\|\phi_{\mathbf{F}}\|_{H^1}^2 = \|\phi_{\mathbf{F}}\|^2 + \|\nabla \phi_{\mathbf{F}}\|^2$, the following result is obvious.

Corollary 2.7. *We have*

$$\|\phi_{\mathbf{F}}\|_{\ell^\infty(0,T;H^1)} := \max_{0 \leq m \leq M} \|\phi_{\mathbf{F}}^m\|_{H^1} \leq \hat{C}_{1,\varepsilon} := C\varepsilon^{-1}, \quad (2.41)$$

in which C is a constant independent of h , Δt , T , and ε .

2.4 Statement of the main theorem

The error estimate for the numerical scheme (2.31) has been reported in [12], with second order accuracy in time and fourth order accuracy in space. However, a standard error estimate using the discrete Gronwall inequality has always contained a convergence constant singularly dependent on ε^{-1} in an exponential form.

A refined error estimate is provided in this article. The following theorem is the main theoretical result.

Theorem 2.8. *Suppose that the initial data ϕ_0 is sufficiently smooth and that Δt and h satisfy the scaling laws*

$$\Delta t \leq \hat{C}\varepsilon^{J_1}, \quad h \leq \hat{C}\varepsilon^{J_2}, \quad (2.42)$$

where J_1 and J_2 are positive integers that are sufficiently large, and \hat{C} is a constant for a fixed final time T . Also assume that $0 < \varepsilon < \varepsilon_0$, with ε_0 specified in Proposition 4.2. Then the following convergence result is valid:

$$\max_{1 \leq m \leq M} \|e^m\|_{-1,h} \leq \hat{R}^*(\Delta t^2 + h^4), \quad \text{with } M = \left\lceil \frac{T}{\Delta t} \right\rceil, \quad \hat{R}^* = C e^{C_0^* T} \varepsilon^{-J_0}, \quad (2.43)$$

where J_0 is a positive integer, C_0^* and C are positive constants that are independent of Δt , h and ε .

3 Higher order Sobolev estimates of the numerical scheme

3.1 $\ell^\infty(0, T; H_h^m)$ ($m \geq 2$) bound of the scheme

A uniform in time H_h^1 bound of the numerical solution has been proved in Theorem 2.6, as presented in [12]. However, such a bound is not sufficient for the desired estimate of a refined convergence constant. In this section, we establish a uniform in time H_h^m bound, for any $m \geq 2$, of the numerical solution. More importantly, the derived bound depends on ε^{-1} in a polynomial form.

Theorem 3.1. *For the proposed numerical scheme (2.31), if $\Delta t \leq \frac{\varepsilon}{2\sqrt{2}A^{\frac{1}{2}}}$, we have*

$$\|\phi_{\mathbf{F}}\|_{\ell^\infty(0,T;H^2)} := \max_{0 \leq m \leq M} \|\phi_{\mathbf{F}}^m\|_{H^2} \leq \hat{C}_{2,\varepsilon} := C\varepsilon^{-k_2}, \quad (3.1)$$

in which k_2 is a positive integer and $C > 0$ is a constant independent of h , Δt , T , and ε .

Proof. Taking the discrete inner product with (2.31) by $2\Delta_{h,(4)}^2 \phi^{n+1}$ gives

$$\begin{aligned} & \langle 3\phi^{n+1} - 4\phi^n + \phi^{n-1}, \Delta_{h,(4)}^2 \phi^{n+1} \rangle + 2\varepsilon \Delta t \|\Delta_{h,(4)}^2 \phi^{n+1}\|_2^2 \\ & + 2A\varepsilon^{-2} \Delta t^2 \langle \Delta_{h,(4)}^2 (\phi^{n+1} - \phi^n), \Delta_{h,(4)}^2 \phi^{n+1} \rangle \\ & = -2\varepsilon^{-1} \Delta t \langle \Delta_{h,(4)} (2\phi^n - \phi^{n-1}), \Delta_{h,(4)}^2 \phi^{n+1} \rangle + 2\varepsilon^{-1} \Delta t \langle \Delta_{h,(4)} (\phi^{n+1})^3, \Delta_{h,(4)}^2 \phi^{n+1} \rangle. \end{aligned} \quad (3.2)$$

The temporal differentiation term could be analyzed as follows, with the help of summation-by-parts formula:

$$\begin{aligned} & \langle 3\phi^{n+1} - 4\phi^n + \phi^{n-1}, \Delta_{h,(4)}^2 \phi^{n+1} \rangle = \langle \Delta_{h,(4)} (3\phi^{n+1} - 4\phi^n + \phi^{n-1}), \Delta_{h,(4)} \phi^{n+1} \rangle \\ & = \frac{1}{2} (\|\Delta_{h,(4)} \phi^{n+1}\|_2^2 - \|\Delta_{h,(4)} \phi^n\|_2^2 + \|\Delta_{h,(4)} (2\phi^{n+1} - \phi^n)\|_2^2 - \|\Delta_{h,(4)} (2\phi^n - \phi^{n-1})\|_2^2 \\ & \quad + \|\Delta_{h,(4)} (\phi^{n+1} - 2\phi^n + \phi^{n-1})\|_2^2). \end{aligned} \quad (3.3)$$

A triangular equality could be applied to the artificial regularization term:

$$2\langle \Delta_{h,(4)}^2(\phi^{n+1} - \phi^n), \Delta_{h,(4)}^2\phi^{n+1} \rangle = \|\Delta_{h,(4)}^2\phi^{n+1}\|_2^2 - \|\Delta_{h,(4)}^2\phi^n\|_2^2 + \|\Delta_{h,(4)}^2(\phi^{n+1} - \phi^n)\|_2^2. \quad (3.4)$$

In terms of the concave diffusion term, we denote $\hat{\phi}^{n+1} = 2\phi^n - \phi^{n-1}$ and see that

$$\begin{aligned} -\langle \Delta_{h,(4)}\hat{\phi}^{n+1}, \Delta_{h,(4)}^2\phi^{n+1} \rangle &\leq \alpha\|\Delta_{h,(4)}^2\phi^{n+1}\|_2^2 + \frac{1}{4\alpha}\|\Delta_{h,(4)}\hat{\phi}^{n+1}\|_2^2 \\ &\leq \alpha\|\Delta_{h,(4)}^2\phi^{n+1}\|_2^2 + \frac{4}{9\alpha}\|\Delta_h\hat{\phi}^{n+1}\|_2^2 \leq \alpha\|\Delta_{h,(4)}^2\phi^{n+1}\|_2^2 + \frac{8}{3\alpha}\|\Delta_h\phi^n\|_2^2 + \frac{4}{3\alpha}\|\Delta_h\phi^{n-1}\|_2^2, \end{aligned} \quad (3.5)$$

for any $\alpha > 0$, in which inequality (2.10) has been applied at the second step. Meanwhile, the quantities $\|\Delta_h\phi^n\|_2^2, \|\Delta_h\phi^{n-1}\|_2^2$ can be controlled by

$$\begin{aligned} \|\Delta_h\phi^\ell\|_2^2 &\leq \|\nabla_h\phi^\ell\|_2^{\frac{4}{3}} \cdot \|\Delta_h^2\phi^\ell\|_2^{\frac{2}{3}} \leq \frac{2}{3\alpha}\|\nabla_h\phi^\ell\|_2^2 + \frac{\alpha^2}{3}\|\Delta_h^2\phi^\ell\|_2^2 \\ &\leq \frac{2}{3\alpha}\|\nabla_h\phi^\ell\|_2^2 + \frac{\alpha^2}{3}\|\Delta_{h,(4)}^2\phi^\ell\|_2^2 \leq \frac{2\tilde{C}_{1,\varepsilon}^2}{3\alpha} + \frac{\alpha^2}{3}\|\Delta_{h,(4)}^2\phi^\ell\|_2^2, \quad \ell = n, n-1, \quad \forall \alpha > 0, \end{aligned} \quad (3.6)$$

in which the first step corresponds to a Sobolev interpolation inequality, the second step comes from an application of Young's inequality, the third step is based on inequality (2.10), and the preliminary H_h^1 estimate (2.40) is recalled in the last step. In turn, a combination of (3.5) and (3.6) leads to

$$-\langle \Delta_{h,(4)}\hat{\phi}^{n+1}, \Delta_{h,(4)}^2\phi^{n+1} \rangle \leq \alpha\|\Delta_{h,(4)}^2\phi^{n+1}\|_2^2 + \frac{8\alpha}{9}\|\Delta_{h,(4)}^2\phi^n\|_2^2 + \frac{4\alpha}{9}\|\Delta_{h,(4)}^2\phi^{n-1}\|_2^2 + \frac{8\tilde{C}_{1,\varepsilon}^2}{3\alpha^2}, \quad (3.7)$$

for any $\alpha > 0$.

Regarding the nonlinear term, we begin with the following observation:

$$\langle \Delta_{h,(4)}(\phi^{n+1})^3, \Delta_{h,(4)}^2\phi^{n+1} \rangle \leq \|\Delta_{h,(4)}(\phi^{n+1})^3\|_2 \cdot \|\Delta_{h,(4)}^2\phi^{n+1}\|_2 \leq \frac{4}{3}\|\Delta_h(\phi^{n+1})^3\|_2 \cdot \|\Delta_{h,(4)}^2\phi^{n+1}\|_2, \quad (3.8)$$

in which inequality (2.10) has been applied again. The rest work is focused on obtaining a bound for $\|\Delta_h(\phi^{n+1})^3\|_2$. Detailed expansions and repeated applications of the discrete Hölder inequality yields the following estimate (also see the derivation in [27]):

$$\begin{aligned} \|\Delta_h(fgh)\|_2 &\leq C\left(\|f\|_\infty \cdot \|g\|_\infty \cdot \|h\|_{H_h^2} + \|f\|_\infty \cdot \|h\|_\infty \cdot \|g\|_{H_h^2} \right. \\ &\quad \left. + \|g\|_\infty \cdot \|h\|_\infty \cdot \|f\|_{H_h^2} + \|f\|_\infty \cdot \|\nabla_h g\|_\infty \cdot \|\nabla_h h\|_2 \right. \\ &\quad \left. + \|g\|_\infty \cdot \|\nabla_h f\|_\infty \cdot \|\nabla_h h\|_2 + \|h\|_\infty \cdot \|\nabla_h f\|_\infty \cdot \|\nabla_h g\|_2\right). \end{aligned} \quad (3.9)$$

In turn, a substitution of $f = g = h = \phi^{n+1}$ gives

$$\|\Delta_h(\phi^{n+1})^3\|_2 \leq C\|\phi^{n+1}\|_\infty \cdot \|\nabla_h\phi^{n+1}\|_\infty \cdot \|\phi^{n+1}\|_{H_h^1} + C\|\phi^{n+1}\|_\infty^2 \cdot \|\phi^{n+1}\|_{H_h^2}. \quad (3.10)$$

The uniform in time H_h^1 estimate (2.40), combined with the 3-D discrete Sobolev inequality (2.13), and the discrete Gagliardo-Nirenberg type inequalities (2.14) and (2.15), yields

$$\|\phi^\ell\|_{H_h^2} \leq C(\|\phi^\ell\|_{H_h^1}^{\frac{2}{3}}\|\Delta_h^2\phi^\ell\|_2^{\frac{1}{3}} + \|\phi^\ell\|_{H_h^1}) \leq C(\tilde{C}_{1,\varepsilon}^{\frac{2}{3}} \cdot \|\Delta_h^2\phi^\ell\|_2^{\frac{1}{3}} + \tilde{C}_{1,\varepsilon}), \quad (3.11)$$

$$\|\phi^\ell\|_\infty \leq C(\|\phi^\ell\|_{H_h^1}^{\frac{5}{6}}\|\Delta_h^2\phi^\ell\|_2^{\frac{1}{6}} + \|\phi^\ell\|_{H_h^1}) \leq C(\tilde{C}_{1,\varepsilon}^{\frac{5}{6}} \cdot \|\Delta_h^2\phi^\ell\|_2^{\frac{1}{6}} + \tilde{C}_{1,\varepsilon}), \quad (3.12)$$

$$\|\nabla_h\phi^\ell\|_\infty \leq C_{11}\|\phi^\ell\|_{H_h^1}^{\frac{1}{2}} \cdot \|\Delta_h^2\phi^\ell\|_2^{\frac{1}{2}} \leq C\tilde{C}_{1,\varepsilon}^{\frac{1}{2}} \cdot \|\Delta_h^2\phi^\ell\|_2^{\frac{1}{2}}, \quad (3.13)$$

for $\ell = n + 1$. Going back (3.10), we obtain

$$\|\Delta_h(\phi^{n+1})^3\|_2 \leq C \left(\tilde{C}_{1,\varepsilon}^{\frac{7}{3}} \cdot \|\Delta_h^2 \phi^{n+1}\|_2^{\frac{2}{3}} + \tilde{C}_{1,\varepsilon}^3 \right) \leq C \left(\tilde{C}_{1,\varepsilon}^{\frac{7}{3}} \cdot \|\Delta_{h,(4)}^2 \phi^{n+1}\|_2^{\frac{2}{3}} + \tilde{C}_{1,\varepsilon}^3 \right), \quad (3.14)$$

with an application of inequality (2.10) in the second step. A combination of (3.14) and (3.8) implies that

$$\begin{aligned} \langle \Delta_{h,(4)}(\phi^{n+1})^3, \Delta_{h,(4)}^2 \phi^{n+1} \rangle &\leq C \left(\tilde{C}_{1,\varepsilon}^{\frac{7}{3}} \cdot \|\Delta_{h,(4)}^2 \phi^{n+1}\|_2^{\frac{5}{3}} + \tilde{C}_{1,\varepsilon}^3 \cdot \|\Delta_{h,(4)}^2 \phi^{n+1}\|_2 \right) \\ &\leq C \alpha^{-5} \tilde{C}_{1,\varepsilon}^{14} + \alpha \|\Delta_{h,(4)}^2 \phi^{n+1}\|_2^2, \quad \forall \alpha > 0, \end{aligned} \quad (3.15)$$

in which the Young's inequality has been applied.

Therefore, a substitution (3.3), (3.4), (3.7) and (3.15) into (3.2) results in

$$\begin{aligned} &\frac{1}{2} (\|\Delta_{h,(4)} \phi^{n+1}\|_2^2 - \|\Delta_{h,(4)} \phi^n\|_2^2 + \|\Delta_{h,(4)}(2\phi^{n+1} - \phi^n)\|_2^2 - \|\Delta_{h,(4)}(2\phi^n - \phi^{n-1})\|_2^2) \\ &\quad + 2A\varepsilon^{-2} \Delta t^2 (\|\Delta_{h,(4)}^2 \phi^{n+1}\|_2^2 - \|\Delta_{h,(4)}^2 \phi^n\|_2^2) + 2(\varepsilon - 2\alpha\varepsilon^{-1}) \Delta t \|\Delta_{h,(4)}^2 \phi^{n+1}\|_2^2 \\ &\leq \frac{16\alpha\varepsilon^{-1} \Delta t}{9} \|\Delta_{h,(4)}^2 \phi^n\|_2^2 + \frac{8\alpha\varepsilon^{-1} \Delta t}{9} \|\Delta_{h,(4)}^2 \phi^{n-1}\|_2^2 + C_{4,\varepsilon} \Delta t, \\ &\text{with } C_{4,\varepsilon} = \frac{16\tilde{C}_{1,\varepsilon}^2 \varepsilon^{-1}}{3\alpha^2} + C\alpha^{-5} \tilde{C}_{1,\varepsilon}^{14} \varepsilon^{-1}. \end{aligned} \quad (3.16)$$

Subsequently, by setting $\alpha = \frac{1}{16}\varepsilon^2$, we get

$$\begin{aligned} &\frac{1}{2} (\|\Delta_{h,(4)} \phi^{n+1}\|_2^2 + \|\Delta_{h,(4)}(2\phi^{n+1} - \phi^n)\|_2^2) + 2A\varepsilon^{-2} \Delta t^2 \|\Delta_{h,(4)}^2 \phi^{n+1}\|_2^2 + \frac{7\varepsilon \Delta t}{4} \|\Delta_{h,(4)}^2 \phi^{n+1}\|_2^2 \\ &\leq \frac{1}{2} (\|\Delta_{h,(4)} \phi^n\|_2^2 + \|\Delta_{h,(4)}(2\phi^n - \phi^{n-1})\|_2^2) + 2A\varepsilon^{-2} \Delta t^2 \|\Delta_{h,(4)}^2 \phi^n\|_2^2 \\ &\quad + \frac{\varepsilon \Delta t}{18} (2\|\Delta_{h,(4)}^2 \phi^n\|_2^2 + \|\Delta_{h,(4)}^2 \phi^{n-1}\|_2^2) + C_{4,\varepsilon} \Delta t. \end{aligned} \quad (3.17)$$

For simplicity, we denote $F^n := \frac{1}{2} (\|\Delta_{h,(4)} \phi^n\|_2^2 + \|\Delta_{h,(4)}(2\phi^n - \phi^{n-1})\|_2^2) + 2A\varepsilon^{-2} \Delta t^2 \|\Delta_{h,(4)}^2 \phi^n\|_2^2$. Meanwhile, an addition of $\frac{2\varepsilon \Delta t}{9} \|\Delta_{h,(4)}^2 \phi^n\|_2^2$ to both sides of the last inequality yields

$$\begin{aligned} &F^{n+1} + \frac{7\varepsilon \Delta t}{4} \|\Delta_{h,(4)}^2 \phi^{n+1}\|_2^2 + \frac{2\varepsilon \Delta t}{9} \|\Delta_{h,(4)}^2 \phi^n\|_2^2 \\ &\leq F^n + \frac{\varepsilon \Delta t}{3} \|\Delta_{h,(4)}^2 \phi^n\|_2^2 + \frac{\varepsilon \Delta t}{18} \|\Delta_{h,(4)}^2 \phi^{n-1}\|_2^2 + C_{4,\varepsilon} \Delta t. \end{aligned} \quad (3.18)$$

In turn, a modified functional quantity is introduced as

$$\begin{aligned} G^n &:= F^n + \frac{\varepsilon \Delta t}{3} \|\Delta_{h,(4)}^2 \phi^n\|_2^2 + \frac{\varepsilon \Delta t}{18} \|\Delta_{h,(4)}^2 \phi^{n-1}\|_2^2 \\ &= \left(\frac{1}{2} + 2A\varepsilon^{-2} \Delta t^2 \right) \|\Delta_{h,(4)} \phi^n\|_2^2 + \frac{1}{2} \|\Delta_{h,(4)}(2\phi^n - \phi^{n-1})\|_2^2 \\ &\quad + \frac{\varepsilon \Delta t}{3} \|\Delta_{h,(4)}^2 \phi^n\|_2^2 + \frac{\varepsilon \Delta t}{18} \|\Delta_{h,(4)}^2 \phi^{n-1}\|_2^2, \end{aligned} \quad (3.19)$$

so that the following inequality is valid:

$$G^{n+1} + \frac{17\varepsilon \Delta t}{12} \|\Delta_{h,(4)}^2 \phi^{n+1}\|_2^2 + \frac{\varepsilon \Delta t}{6} \|\Delta_{h,(4)}^2 \phi^n\|_2^2 \leq G^n + C_{4,\varepsilon} \Delta t. \quad (3.20)$$

On the other hand, the following estimates could be derived, with the help of inequality (2.19):

$$\begin{aligned} \left(\frac{1}{2} + 2A\varepsilon^{-2}\Delta t^2\right)\|\Delta_{h,(4)}\phi^{n+1}\|_2^2 &\leq \frac{3}{4}\|\Delta_{h,(4)}\phi^{n+1}\|_2^2 \leq \frac{3}{4}C_1^2\|\Delta_{h,(4)}^2\phi^{n+1}\|_2^2, \text{ if } \Delta t \leq \frac{\varepsilon}{2\sqrt{2}A^{\frac{1}{2}}}, \\ \frac{1}{2}\|\Delta_{h,(4)}(2\phi^{n+1} - \phi^n)\|_2^2 &\leq 3\|\Delta_{h,(4)}\phi^{n+1}\|_2^2 + \frac{3}{2}\|\Delta_{h,(4)}\phi^n\|_2^2 \\ &\leq 3C_1^2\|\Delta_{h,(4)}^2\phi^{n+1}\|_2^2 + \frac{3C_1^2}{2}\|\Delta_{h,(4)}^2\phi^n\|_2^2, \end{aligned}$$

$$\begin{aligned} \text{so that } G^{n+1} &= \left(\frac{1}{2} + 2A\varepsilon^{-2}\Delta t^2\right)\|\Delta_{h,(4)}\phi^{n+1}\|_2^2 + \frac{1}{2}\|\Delta_{h,(4)}(2\phi^{n+1} - \phi^n)\|_2^2 \\ &\quad + \frac{\varepsilon\Delta t}{3}\|\Delta_{h,(4)}^2\phi^{n+1}\|_2^2 + \frac{\varepsilon\Delta t}{18}\|\Delta_{h,(4)}^2\phi^n\|_2^2 \\ &\leq 4C_1^2\|\Delta_{h,(4)}^2\phi^{n+1}\|_2^2 + 2C_1^2\|\Delta_{h,(4)}^2\phi^n\|_2^2, \text{ if } \Delta t \leq \frac{3}{4}C_1^2\varepsilon^{-1}, \end{aligned} \quad (3.21)$$

$$\text{and } \frac{17\varepsilon\Delta t}{12}\|\Delta_{h,(4)}^2\phi^{n+1}\|_2^2 + \frac{\varepsilon\Delta t}{6}\|\Delta_{h,(4)}^2\phi^n\|_2^2 \geq \frac{\varepsilon\Delta t}{12C_1^2}G^{n+1} + \varepsilon\Delta t\|\Delta_{h,(4)}^2\phi^{n+1}\|_2^2.$$

Going back (3.20), we arrive at

$$\left(1 + \frac{\varepsilon\Delta t}{12C_1^2}\right)G^{m+1} + \varepsilon\Delta t\|\Delta_{h,(4)}^2\phi^{n+1}\|_2^2 \leq G^m + C_{4,\varepsilon}\Delta t. \quad (3.22)$$

An application of recursive argument to the above inequality reveals that

$$\begin{aligned} G^{m+1} &\leq \left(1 + \frac{\varepsilon^2\Delta t}{12C_1^2}\right)^{-(n+1)}G^0 + 12C_1^2\varepsilon^{-1}C_{4,\varepsilon} \leq G^0 + 12C_1^2\varepsilon^{-1}C_{4,\varepsilon}, \text{ so that} \\ \|\Delta_h\phi^{n+1}\|_2^2 &\leq \|\Delta_{h,(4)}\phi^{n+1}\|_2^2 \leq 2G^{n+1} \leq 2(G^0 + 12C_1^2\varepsilon^{-1}C_{4,\varepsilon}), \quad \forall n \geq 0. \end{aligned} \quad (3.23)$$

As a consequence, (3.1) is a direct consequence of (3.23) and the elliptic regularity:

$$\begin{aligned} \|\phi_{\mathbf{F}}^{n+1}\|_{H^2} &\leq C(\|\phi_{\mathbf{F}}^{n+1}\| + \|\Delta_h\phi_{\mathbf{F}}^{n+1}\|) \leq C\left(\hat{C}_{1,\varepsilon} + \|\Delta_h\phi^{n+1}\|_2\right) \\ &\leq C(\hat{C}_{1,\varepsilon} + (2G^{n+1})^{\frac{1}{2}}) \leq C(\hat{C}_{1,\varepsilon} + \sqrt{2}(G^0)^{1/2} + 2\sqrt{6}C_1C_{4,\varepsilon}^{\frac{1}{2}}\varepsilon^{-\frac{1}{2}}) := \hat{C}_{2,\varepsilon}, \end{aligned} \quad (3.24)$$

in which inequality (2.16) has been applied in the second step. It is clear that $\hat{C}_{2,\varepsilon}$ depends on ε^{-1} in a polynomial form, since $C_{4,\varepsilon}$ does. The proof of Theorem 3.1 is complete. \square

Using numerical analysis techniques, a uniform in time H^{m_0} bound for the numerical solution could be established, for any $m_0 \geq 2$. To obtain such a bound, a discrete inner product with (2.31) is taken by $(-\Delta_{h,(4)})^{m_0}\phi^{n+1}$, and repeated application of discrete Hölder inequality, Sobolev embedding, as well as Gagliardo-Nirenberg inequality, will play a crucial role in the derivation. The details are left for interested readers.

Theorem 3.2. *For the proposed numerical scheme (2.31), if $\Delta t \leq C\varepsilon$, we have*

$$\|\phi_{\mathbf{F}}\|_{\ell^\infty(0,T;H^{m_0})} := \max_{0 \leq m \leq M} \|\phi_{\mathbf{F}}^m\|_{H^{m_0}} \leq \hat{C}_{m_0,\varepsilon} := C\varepsilon^{-k_{m_0}}, \quad (3.25)$$

where k_{m_0} is a positive integer and $C > 0$ is a constant independent of h , Δt , T , and ε .

3.2 A uniform estimate for $\|\phi^{n+1} - \phi^n\|_{H_h^k}$

The following estimate is needed in the later analysis.

Theorem 3.3. *For the proposed numerical scheme (2.31), if $\Delta t \leq C\varepsilon$, we have*

$$\max_{0 \leq n \leq M-1} \|\phi_{\mathbf{F}}^{n+1} - \phi_{\mathbf{F}}^n\|_{H^k} \leq \hat{D}_{k,\varepsilon} \Delta t, \quad \text{with } \hat{D}_{k,\varepsilon} := C\varepsilon^{-n_k}, \quad (3.26)$$

where n_k is a positive integer and $C > 0$ is a constant independent of h , Δt , T , and ε .

Proof. A careful evaluation of the numerical scheme (2.31) indicates that

$$\left\| \left(\frac{3}{2} \phi^{n+1} - 2\phi^n + \frac{1}{2} \phi^{n-1} \right)_{\mathbf{F}} \right\|_{H^k} = \Delta t \|(\Delta_{h,(4)} \mu^{n+1})_{\mathbf{F}}\|_{H^k} \leq \Delta t \|\Delta(\mu^{n+1})_{\mathbf{F}}\|_{H^k}, \quad (3.27)$$

in which the last step comes from estimate (2.20)). On the other hand, the term $(\mu^{n+1})_{\mathbf{F}}$ has the following expansion:

$$(\mu^{n+1})_{\mathbf{F}} = \varepsilon^{-1} \left(\mathcal{I}_N(\phi_{\mathbf{F}}^{n+1})^3 - \hat{\phi}_{\mathbf{F}}^{n+1} \right) - \varepsilon(\Delta_{h,(4)} \phi^{n+1})_{\mathbf{F}} - A\varepsilon^{-2} \Delta t (\Delta_{h,(4)} (\phi^{n+1} - \phi^n))_{\mathbf{F}}, \quad (3.28)$$

with $\hat{\phi}_{\mathbf{F}}^{n+1} = 2\phi_{\mathbf{F}}^n - \phi_{\mathbf{F}}^{n-1}$. Moreover, with the help of the uniform in time estimates (3.25), combined with repeated applications of Hölder inequality and Sobolev embedding, we are able to derive the following estimates:

$$\|\Delta(\mathcal{I}_N(\phi_{\mathbf{F}}^{n+1})^3)\|_{H^k} \leq C \|(\phi_{\mathbf{F}}^{n+1})^3\|_{H^{k+2}} \leq C \|\phi_{\mathbf{F}}^{n+1}\|_{H^{k+2}}^3 \leq C \hat{C}_{k+2,\varepsilon}^3, \quad (3.29)$$

$$\|\Delta \hat{\phi}_{\mathbf{F}}^{n+1}\|_{H^k} \leq C (\|\phi_{\mathbf{F}}^n\|_{H^{k+2}} + \|\phi_{\mathbf{F}}^{n-1}\|_{H^{k+2}}) \leq C \hat{C}_{k+2,\varepsilon}, \quad (3.30)$$

$$\begin{aligned} \|\Delta(\Delta_{h,(4)} \phi^\ell)_{\mathbf{F}}\|_{H^k} &\leq \|(\Delta_{h,(4)} \hat{\phi}^\ell)_{\mathbf{F}}\|_{H^{k+2}} \leq \|\Delta \phi_{\mathbf{F}}^\ell\|_{H^{k+2}} \\ &\leq C \|\phi_{\mathbf{F}}^\ell\|_{H^{k+4}} \leq C \hat{C}_{k+4,\varepsilon}, \quad \ell = n, n+1, \end{aligned} \quad (3.31)$$

In fact, inequality (2.20) has been applied again in the second step of (3.31). In turn, a substitution of (3.29)-(3.31) into (3.28) and (3.27) leads to

$$\left\| \left(\frac{3}{2} \phi^{n+1} - 2\phi^n + \frac{1}{2} \phi^{n-1} \right)_{\mathbf{F}} \right\|_{H^k} \leq D_{k,\varepsilon}^{(1)} \Delta t, \quad D_{k,\varepsilon}^{(1)} = C \left(\varepsilon^{-1} (\hat{C}_{k+2,\varepsilon}^3 + \hat{C}_{k+2,\varepsilon}) + \varepsilon \hat{C}_{k+4,\varepsilon} \right). \quad (3.32)$$

It is clear that $D_{k,\varepsilon}^{(1)}$ is a uniform-in-time constant, and it depends on ε^{-1} in a polynomial form, since both $\hat{C}_{k+2,\varepsilon}$ and $\hat{C}_{k+4,\varepsilon}$ do.

Meanwhile, a further estimate is needed to obtain a uniform estimate for $\|(\phi^{n+1} - \phi^n)_{\mathbf{F}}\|_{H^k}$. Motivated by the triangular inequality

$$\left\| \left(\frac{3}{2} \phi^{n+1} - 2\phi^n + \frac{1}{2} \phi^{n-1} \right)_{\mathbf{F}} \right\|_{H^k} \geq \frac{3}{2} \|(\phi^{n+1} - \phi^n)_{\mathbf{F}}\|_{H^k} - \frac{1}{2} \|(\phi^n - \phi^{n-1})_{\mathbf{F}}\|_{H^k}, \quad (3.33)$$

we see that

$$\|(\phi^{n+1} - \phi^n)_{\mathbf{F}}\|_{H^k} \leq \frac{2}{3} D_{k,\varepsilon}^{(1)} \Delta t + \frac{1}{3} \|(\phi^n - \phi^{n-1})_{\mathbf{F}}\|_{H^k}. \quad (3.34)$$

In turn, a recursive argument to the above inequality implies that

$$\|(\phi^{n+1} - \phi^n)_{\mathbf{F}}\|_{H^k} \leq D_{k,\varepsilon}^{(1)} \Delta t + \left(\frac{1}{3}\right)^n \|(\phi^0 - \phi^{-1})_{\mathbf{F}}\|_{H^k} \leq (D_{k,\varepsilon}^{(1)} + C^*) \Delta t, \quad \forall n \geq 0, \quad (3.35)$$

in which C^* is related to the initialization data (2.36). This finishes the proof of Theorem 3.3, by taking $\hat{D}_{k,\varepsilon} = D_{k,\varepsilon}^{(1)} + C^*$. \square

3.3 A uniform estimate for $\|\phi^{n+1} - 2\phi^n + \phi^{n-1}\|_{H_h^k}$

In addition to the first order temporal difference operator, the second order differential stencil term, namely $\phi^{n+1} - 2\phi^n + \phi^{n-1}$, needs to be analyzed in the BDF2 scheme. A uniform-in-time estimate is presented in the following theorem.

Theorem 3.4. *For the proposed numerical scheme (2.31), if $\Delta t \leq C\varepsilon^{\frac{1}{2}}$, we have*

$$\max_{1 \leq n \leq M-1} \|\phi_{\mathbf{F}}^{n+1} - 2\phi_{\mathbf{F}}^n + \phi_{\mathbf{F}}^{n-1}\|_{H^k} \leq \hat{Q}_{k,\varepsilon} \Delta t^2, \quad \text{with } \hat{Q}_{k,\varepsilon} := C\varepsilon^{-m_k}, \quad (3.36)$$

where m_k is a positive integer and $C > 0$ is a constant independent of h , Δt , T , and ε .

Proof. Taking a difference between $\frac{3}{2}\phi_{\mathbf{F}}^{n+1} - 2\phi_{\mathbf{F}}^n + \frac{1}{2}\phi_{\mathbf{F}}^{n-1}$ and $\frac{3}{2}\phi_{\mathbf{F}}^n - 2\phi_{\mathbf{F}}^{n-1} + \frac{1}{2}\phi_{\mathbf{F}}^{n-2}$, evaluated by the numerical algorithm (2.31) at time steps t^{n+1} , t^n , respectively, gives

$$\begin{aligned} & \left\| \left(\frac{3}{2}\phi^{n+1} - \frac{7}{2}\phi^n + \frac{5}{2}\phi^{n-1} - \frac{1}{2}\phi^{n-2} \right)_{\mathbf{F}} \right\|_{H^k} = \Delta t \left\| (\Delta_{h,(4)}(\mu^{n+1} - \mu^n))_{\mathbf{F}} \right\|_{H^k} \\ & \leq \Delta t \left\| \Delta(\mu^{n+1} - \mu^n)_{\mathbf{F}} \right\|_{H^k}, \quad \text{with} \end{aligned} \quad (3.37)$$

$$\begin{aligned} \mu^{n+1} - \mu^n &= \varepsilon^{-1} \left((\phi^{n+1})^3 - (\phi^n)^3 - 2(\phi^n - \phi^{n-1}) + (\phi^{n-1} - \phi^{n-2}) \right) \\ & \quad - \varepsilon \Delta_{h,(4)}(\phi^{n+1} - \phi^n) - A\varepsilon^{-2} \Delta t (\Delta_{h,(4)}(\phi^{n+1} - \phi^n) - \Delta_{h,(4)}(\phi^n - \phi^{n-1})), \end{aligned} \quad (3.38)$$

$$(\phi^{n+1})^3 - (\phi^n)^3 = ((\phi^{n+1})^2 + \phi^{n+1}\phi^n + (\phi^n)^2)(\phi^{n+1} - \phi^n). \quad (3.39)$$

It is observed that all the right-hand-side terms in (3.38) contain a factor of $\phi^\ell - \phi^{\ell-1}$, $n-1 \leq \ell \leq n+1$. In turn, with the help of (3.25) and (3.26), the following estimate could be carefully derived; the technical details are skipped for the sake of brevity:

$$\left\| \left(\frac{3}{2}\phi^{n+1} - \frac{7}{2}\phi^n + \frac{5}{2}\phi^{n-1} - \frac{1}{2}\phi^{n-2} \right)_{\mathbf{F}} \right\|_{H^k} \leq \Delta t \left\| \Delta(\mu^{n+1} - \mu^n)_{\mathbf{F}} \right\|_{H^k} \leq Q_{k,\varepsilon}^{(1)} \Delta t^2, \quad (3.40)$$

with the uniform-in-time constant $Q_{k,\varepsilon}^{(1)}$ dependent on ε^{-1} in a polynomial form.

To obtain a useful bound for $\phi^{n+1} - 2\phi^n + \phi^{n-1}$, we begin with the following observation:

$$\begin{aligned} & \left\| \left(\frac{3}{2}\phi^{n+1} - \frac{7}{2}\phi^n + \frac{5}{2}\phi^{n-1} - \frac{1}{2}\phi^{n-2} \right)_{\mathbf{F}} \right\|_{H^k} \\ &= \left\| \frac{3}{2}(\phi^{n+1} - 2\phi^n + \phi^{n-1})_{\mathbf{F}} - \frac{1}{2}(\phi^n - 2\phi^{n-1} + \phi^{n-2})_{\mathbf{F}} \right\|_{H^k} \\ &\geq \frac{3}{2} \left\| (\phi^{n+1} - 2\phi^n + \phi^{n-1})_{\mathbf{F}} \right\|_{H^k} - \frac{1}{2} \left\| (\phi^n - 2\phi^{n-1} + \phi^{n-2})_{\mathbf{F}} \right\|_{H^k}. \end{aligned} \quad (3.41)$$

Its combination with (3.40) results in

$$\left\| (\phi^{n+1} - 2\phi^n + \phi^{n-1})_{\mathbf{F}} \right\|_{H^k} \leq \frac{2}{3} Q_{k,\varepsilon}^{(1)} \Delta t^2 + \frac{1}{3} \left\| (\phi^n - 2\phi^{n-1} + \phi^{n-2})_{\mathbf{F}} \right\|_{H^k}. \quad (3.42)$$

Similarly, a recursive argument to this inequality leads to

$$\left\| (\phi^{n+1} - 2\phi^n + \phi^{n-1})_{\mathbf{F}} \right\|_{H^k} \leq Q_{k,\varepsilon}^{(1)} \Delta t^2 + \left(\frac{1}{3} \right)^{n-1} \left\| (\phi^1 - 2\phi^0 + \phi^{-1})_{\mathbf{F}} \right\|_{H^k} \leq (Q_{k,\varepsilon}^{(1)} + C^{**}) \Delta t^2, \quad (3.43)$$

for any $n \geq 1$, in which C^{**} is related to the initialization data of ϕ^1 , ϕ^0 and ϕ^{-1} , with ϕ^{-1} gives by (2.36). This finishes the proof of Theorem 3.4, by taking $\hat{Q}_{k,\varepsilon} = Q_{k,\varepsilon}^{(1)} + C^{**}$. \square

Remark 3.5. *If the Crank-Nicolson-style temporal discretization is applied, the associated uniform-in-time estimates for $\|\phi_{\mathbf{F}}^{n+1} - \phi_{\mathbf{F}}^n\|_{H^k}$ and $\|\phi_{\mathbf{F}}^{n+1} - 2\phi_{\mathbf{F}}^n + \phi_{\mathbf{F}}^{n-1}\|_{H^k}$ could be carried out in a more straightforward way, because of the simpler temporal stencil of $\phi^{n+1} - \phi^n$; see the detailed analysis in [28]. In comparison, if a BDF temporal stencil is applied, a direct control of $\|\phi_{\mathbf{F}}^{n+1} - \phi_{\mathbf{F}}^n\|_{H^k}$ is not available any more. Instead, we have to make use of the triangular inequalities (3.33), (3.41), which come from the original numerical algorithm. These inequalities in turn enable us to derive the desired uniform-in-time bounds (3.35), (3.43), using a recursive argument. This subtle technique could be applied to many other BDF-style, energy stable numerical schemes for various gradient flow models [14, 19, 29, 31, 35, 51], etc.*

3.4 Some established estimates for the exact solution and projection solution

For the exact solution Φ and the projection solution Φ_N , the following estimates could be derived by the energy estimate and Sobolev analysis; also see the relevant reference work [28].

Theorem 3.6. [28] *The following estimates are valid for the exact solution Φ :*

$$\|\Phi\|_{L^\infty(0,T;H^{m_0})} \leq \hat{C}_{m_0,\varepsilon}^* := C\varepsilon^{-k_{m_0}}, \quad \forall m_0 \geq 1, \quad (3.44)$$

$$\|\partial_t \Phi\|_{L^\infty(0,T;H^k)} \leq \hat{D}_{k,\varepsilon}^*, \quad \text{with } \hat{D}_{k,\varepsilon}^* := C\varepsilon^{-n_k}, \quad \forall k \geq 0, \quad (3.45)$$

$$\|\partial_t^2 \Phi\|_{L^\infty(0,T;H^k)} \leq \hat{Q}_{k,\varepsilon}^*, \quad \text{with } \hat{Q}_{k,\varepsilon}^* := C\varepsilon^{-m_k}, \quad \forall k \geq 0, \quad (3.46)$$

$$\max_{0 \leq n \leq M} \|\Phi_N^n\|_{H^{m_0}} \leq \hat{C}_{m_0,\varepsilon}^* := C\varepsilon^{-k_{m_0}}, \quad (3.47)$$

$$\max_{0 \leq n \leq M-1} \|\Phi_N^{n+1} - \Phi_N^n\|_{H^k} \leq \hat{D}_{k,\varepsilon}^* \Delta t, \quad \hat{D}_{k,\varepsilon}^* := C\varepsilon^{-n_k}, \quad (3.48)$$

$$\max_{1 \leq n \leq M-1} \|\Phi_N^{n+1} - 2\Phi_N^n + \Phi_N^{n-1}\|_{H^k} \leq \hat{Q}_{k,\varepsilon}^* \Delta t^2, \quad \hat{Q}_{k,\varepsilon}^* := C\varepsilon^{-m_k}, \quad (3.49)$$

where k_{m_0} , n_k and m_k are given integers and C is a constant independent of h , Δt , T , and ε .

4 Error analysis with a refined convergence constant

With the help of the preliminary estimates for the numerical solution, established in the last section, we are able to establish an improved convergence analysis.

4.1 Consistency analysis and the numerical error evolutionary equation

For the projection solution Φ_N , the following estimate is valid:

$$\partial_t \Phi_N = \Delta (\varepsilon^{-1}(\Phi_N^3 - \Phi_N) - \varepsilon \Delta \Phi_N) + \tau_0, \quad \text{with } \|\tau_0(t)\|_{H_{\text{per}}^{-1}} \leq Ch^m \varepsilon^{-j_1}, \quad (4.1)$$

in which the projection approximation estimates (2.26), (2.28), combined with the exact CH equation (1.2), have to be applied in the derivation.

If the fourth order long stencil difference approximation is taken in space, the following estimate is available:

$$\partial_t \Phi_N = \Delta_{h,(4)} (\varepsilon^{-1}(\Phi_N^3 - \Phi_N) - \varepsilon \Delta_{h,(4)} \Phi_N) + \tau_1, \quad \text{with } \|\tau_1(t)\|_{-1,h} \leq Ch^4 \varepsilon^{-j_2}.$$

Moreover, by taking a modified BDF2 temporal discretization, we have

$$\begin{aligned} \frac{\frac{3}{2}\Phi_N^{n+1} - 2\Phi_N^n + \frac{1}{2}\Phi_N^{n-1}}{\Delta t} &= \Delta_{h,(4)} \left(\varepsilon^{-1} ((\Phi_N^{n+1})^3 - \hat{\Phi}_N^{n+1}) - \varepsilon \Delta_{h,(4)} \Phi_N^{n+1} \right. \\ &\quad \left. + A\varepsilon^{-2} \Delta t \Delta_{h,(4)} (\Phi_N^{n+1} - \Phi_N^n) \right) + \tau^{n+1}, \end{aligned} \quad (4.2)$$

with $\hat{\Phi}_N^{n+1} = 2\Phi_N^n - \Phi_N^{n-1}$, $\|\tau^{n+1}\|_{-1,h} \leq C(\Delta t^2 + h^4)\varepsilon^{-j_3}$.

In turn, subtracting the consistency estimate (4.2) from the numerical scheme (2.31) gives

$$\begin{aligned} \frac{\frac{3}{2}e^{n+1} - 2e^n + \frac{1}{2}e^{n-1}}{\Delta t} &= \Delta_{h,(4)} \left(\varepsilon^{-1} ((\Phi_N^{n+1})^3 - (\phi^{n+1})^3 - \hat{e}^{n+1}) - \varepsilon \Delta_{h,(4)} e^{n+1} \right. \\ &\quad \left. + A\varepsilon^{-2} \Delta t \Delta_{h,(4)} (e^{n+1} - e^n) \right) + \tau^{n+1}, \end{aligned} \quad (4.3)$$

with $\hat{e}^{n+1} = 2e^n - e^{n-1}$, $\|\tau^{n+1}\|_{-1,h} \leq C(\Delta t^2 + h^4)\varepsilon^{-j_4}$.

Meanwhile, it is noticed that the numerical error functions are discrete, and they are only evaluated at the numerical grid points. Using the tool of (2.11) and (2.12), we make a continuous extension of these discrete error functions:

$$e_{\mathbf{F}}^k = \Phi_N^k - \phi_{\mathbf{F}}^k, \quad \hat{e}_{\mathbf{F}}^{k+1} = 2e_{\mathbf{F}}^k - e_{\mathbf{F}}^{k-1}. \quad (4.4)$$

Meanwhile, a few preliminary estimates for the numerical error term will be needed in the later analysis. By making a comparison between (3.25), (3.26), (3.36) and (3.47)-(3.49), the following results become straightforward.

Lemma 4.1. *For the numerical error function, we have*

$$\max_{0 \leq n \leq M} \|e_{\mathbf{F}}^n\|_{H^{m_0}} \leq \hat{C}_{m_0, \varepsilon}^{**} := C\varepsilon^{-k_{m_0}}, \quad (4.5)$$

$$\max_{0 \leq n \leq M-1} \|e_{\mathbf{F}}^{n+1} - e_{\mathbf{F}}^n\|_{H^k} \leq \hat{D}_{k, \varepsilon}^{**} \Delta t, \quad \hat{D}_{k, \varepsilon}^{**} := C\varepsilon^{-n_k}, \quad (4.6)$$

$$\max_{1 \leq n \leq M-1} \|e_{\mathbf{F}}^{n+1} - 2e_{\mathbf{F}}^n + e_{\mathbf{F}}^{n-1}\|_{H^k} \leq \hat{Q}_{k, \varepsilon}^{**} \Delta t^2, \quad \hat{Q}_{k, \varepsilon}^{**} := C\varepsilon^{-m_k}, \quad (4.7)$$

for any $m_0 \geq 1$ and $k \geq 0$, where k_{m_0} , n_k and m_k are given integers and C is a constant independent of h , Δt , T , and ε .

In fact, these preliminary bounds for the numerical error function do not rely on the error and convergence analysis, and all the constants are final time independent.

4.2 Review of the spectrum estimate for the linearized Cahn-Hilliard operator

The following linearized spectrum estimate has been established in [1, 2, 8, 22]. We just recall this result.

Proposition 4.2. ([22]) *There exists $0 < \varepsilon_0 \ll 1$ and another positive constant C_0 such that the principle eigenvalue of the linearized Cahn-Hilliard operator satisfies*

$$\lambda_{CH} := \inf_{\psi \in H^1, \psi \neq 0} \frac{\varepsilon^{-1} ((3\Phi^2(t) - 1)\psi, \psi) + \varepsilon \|\nabla \psi\|^2}{\|\psi\|_{H^{-1}}^2} \geq -C_0, \quad (4.8)$$

for any $t \geq 0$, $0 < \varepsilon < \varepsilon_0$, where Φ is the exact solution to the Cahn-Hilliard problem.

4.3 Proof of Theorem 2.8

Since the numerical error function is mean free, i.e., $\overline{e^k} = 0$, its $\|\cdot\|_{-1,h}$ norm is well defined. Taking a discrete inner product with (4.3) by $2(-\Delta_{h,(4)})^{-1}e^{n+1}$ yields

$$\begin{aligned} & \frac{1}{\Delta t} \left\langle 3e^{n+1} - 4e^n + e^{n-1}, (-\Delta_{h,(4)})^{-1}e^{n+1} \right\rangle + 2\varepsilon^{-1} \langle ((\Phi_N^{n+1})^3 - (\phi^{n+1})^3 - \hat{e}^{n+1}), e^{n+1} \rangle \\ & - 2\varepsilon \langle \Delta_{h,(4)}e^{n+1}, e^{n+1} \rangle - 2A\varepsilon^{-2} \langle \Delta_{h,(4)}(e^{n+1} - e^n), e^{n+1} \rangle = 2\langle \tau^{n+1}, (-\Delta_{h,(4)})^{-1}e^{n+1} \rangle, \end{aligned} \quad (4.9)$$

in which the summation by parts formula has been repeatedly applied.

The analysis for the temporal differentiation term is similar to (3.3):

$$\begin{aligned} & \langle 3e^{n+1} - 4e^n + e^{n-1}, (-\Delta_{h,(4)})^{-1}e^{n+1} \rangle = \langle 3e^{n+1} - 4e^n + e^{n-1}, e^{n+1} \rangle_{-1,h} \\ & = \frac{1}{2} (\|e^{n+1}\|_{-1,h}^2 - \|e^n\|_{-1,h}^2 + \|2e^{n+1} - e^n\|_{-1,h}^2 - \|2e^n - e^{n-1}\|_{-1,h}^2 \\ & \quad + \|e^{n+1} - 2e^n + e^{n-1}\|_{-1,h}^2). \end{aligned} \quad (4.10)$$

The local truncation error term could be bounded in a straightforward way:

$$\begin{aligned} 2\langle \tau^{n+1}, (-\Delta_{h,(4)})^{-1}e^{n+1} \rangle & = 2\langle \tau^{n+1}, e^{n+1} \rangle_{-1,h} \leq 2\|\tau^{n+1}\|_{-1,h} \cdot \|e^{n+1}\|_{-1,h} \\ & \leq \|\tau^{n+1}\|_{-1,h}^2 + \|e^{n+1}\|_{-1,h}^2. \end{aligned} \quad (4.11)$$

For the surface diffusion term, we apply the summation-by-parts formula (2.5), as well as inequality (2.21) (in Lemma 2.4), and get

$$-\langle \Delta_{h,(4)}e^{n+1}, e^{n+1} \rangle = \|\nabla_{h,(4)}e^{n+1}\|_2^2, \quad (4.12)$$

$$\|\nabla e_{\mathbf{F}}^{n+1}\|_2^2 - \|\nabla_{h,(4)}e^{n+1}\|_2^2 \leq Ch^4 \|e_{\mathbf{F}}^{n+1}\|_{H^3}^2. \quad (4.13)$$

On the other hand, the following Sobolev interpolation inequality could be used to obtain a sharper bound on the right hand side:

$$\|e_{\mathbf{F}}^{n+1}\|_{H^3}^2 \leq C\|\nabla \Delta e_{\mathbf{F}}^{n+1}\|_2^2 \leq C\|e_{\mathbf{F}}^{n+\frac{1}{2}}\|_{H^7} \cdot \|e_{\mathbf{F}}^{n+\frac{1}{2}}\|_{H^{-1}} \leq C\hat{C}_{7,\varepsilon}^{**} \|e_{\mathbf{F}}^{n+\frac{1}{2}}\|_{H^{-1}}, \quad (4.14)$$

with the preliminary estimate (4.5) (in Lemma 4.1) applied in the last step. Then we obtain

$$\|\nabla e_{\mathbf{F}}^{n+1}\|_2^2 - \|\nabla_{h,(4)}e^{n+1}\|_2^2 \leq C\hat{C}_{7,\varepsilon}^{**} h^4 \|e_{\mathbf{F}}^{n+1}\|_{H^{-1}} \leq \|e_{\mathbf{F}}^{n+1}\|_{H^{-1}}^2 + Ch^8 (\hat{C}_{7,\varepsilon}^{**})^2, \quad (4.15)$$

$$\text{so that } -\langle \Delta_{h,(4)}e^{n+1}, e^{n+1} \rangle \geq \|\nabla e_{\mathbf{F}}^{n+1}\|_2^2 - Ch^8 (\hat{C}_{7,\varepsilon}^{**})^2. \quad (4.16)$$

Similar to (3.4), the artificial regularization inner product term satisfies the following triangular equality:

$$-2\langle \Delta_{h,(4)}(e^{n+1} - e^n), e^{n+1} \rangle = \|\nabla_{h,(4)}e^{n+1}\|_2^2 - \|\nabla_{h,(4)}e^n\|_2^2 + \|\nabla_{h,(4)}(e^{n+1} - e^n)\|_2^2. \quad (4.17)$$

For the concave term, we begin with the following observation:

$$\begin{aligned} \langle -\hat{e}^{n+1}, e^{n+1} \rangle & = -\|e^{n+1}\|_2^2 + \langle e^{n+1} - 2e^n + e^{n-1}, e^{n+1} \rangle \\ & = -\|e_{\mathbf{F}}^{n+1}\|_2^2 + (e_{\mathbf{F}}^{n+1} - 2e_{\mathbf{F}}^n + e_{\mathbf{F}}^{n-1}, e_{\mathbf{F}}^{n+1}), \end{aligned} \quad (4.18)$$

in which identity (2.29) (in Lemma 2.5) has been applied in the second step. Meanwhile, the second term on the right hand side could be analyzed as follows:

$$\begin{aligned} |(e_{\mathbf{F}}^{n+1} - 2e_{\mathbf{F}}^n + e_{\mathbf{F}}^{n-1}, e_{\mathbf{F}}^{n+1})| & \leq \|\nabla(e_{\mathbf{F}}^{n+1} - 2e_{\mathbf{F}}^n + e_{\mathbf{F}}^{n-1})\| \cdot \|e_{\mathbf{F}}^{n+1}\|_{H^{-1}} \\ & \leq \hat{Q}_{1,\varepsilon}^{**} \Delta t^2 \cdot \|e_{\mathbf{F}}^{n+1}\|_{H^{-1}} \leq \frac{\varepsilon}{2} \|e_{\mathbf{F}}^{n+1}\|_{H^{-1}}^2 + \frac{1}{2} \varepsilon^{-1} (\hat{Q}_{1,\varepsilon}^{**})^2 \Delta t^4, \end{aligned} \quad (4.19)$$

where the second step comes from the preliminary estimate (4.7) (in Lemma 4.1). Then we arrive at a bound for the concave term:

$$2\varepsilon^{-1}\langle -\hat{e}^{n+1}, e^{n+1} \rangle \geq -2\varepsilon^{-1}\|e_{\mathbf{F}}^{n+1}\|^2 - \|e_{\mathbf{F}}^{n+1}\|_{H^{-1}}^2 - \varepsilon^{-2}(\hat{Q}_{1,\varepsilon}^{**})^2\Delta t^4. \quad (4.20)$$

The rest work is focused on the nonlinear estimate. The following a-priori assumption is made. **An a-priori assumption up to time step t^n .** We assume a-priori that the numerical error function has the following convergence order, at time steps up to t^n :

$$\|e^\ell\|_{-1,h} \leq \Delta t^{\frac{15}{8}} + h^{\frac{15}{4}}, \quad \ell \leq n. \quad (4.21)$$

First, the nonlinear error inner product could be expanded as

$$I_1^{(d)} := \langle (\Phi_N^{n+1})^3 - (\phi^{n+1})^3, e^{n+1} \rangle = \left\langle \left((\Phi_N^{n+1})^2 + \Phi_N^{n+1}\phi^{n+1} + (\phi^{n+1})^2 \right), (e^{n+1})^2 \right\rangle. \quad (4.22)$$

To bound this nonlinear inner product, we make use of (2.30) (in Lemma 2.5) to control its difference with its continuous version:

$$I_1 := \left\langle \left((\Phi_N^{n+1})^2 + \Phi_N^{n+1}\phi_{\mathbf{F}}^{n+1} + (\phi_{\mathbf{F}}^{n+1})^2 \right), (e_{\mathbf{F}}^{n+1})^2 \right\rangle, \quad (4.23)$$

$$\begin{aligned} |I_1^{(d)} - I_1| &\leq Ch^8 \left(\|(\Phi_N^{n+1})^2 + \Phi_N^{n+1}\phi_{\mathbf{F}}^{n+1} + (\phi_{\mathbf{F}}^{n+1})^2\|_{H^8} \cdot \|(e_{\mathbf{F}}^{n+1})^2\|_{H^8} \right) \\ &\leq Ch^8 \left(\left(\|\Phi_N^{n+1}\|_{H^8}^2 + \|\phi_{\mathbf{F}}^{n+1}\|_{H^8}^2 \right) \cdot \|e_{\mathbf{F}}^{n+1}\|_{H^8}^2 \right) \\ &\leq Ch^8 \left(\hat{C}_{8,\varepsilon}^4 + (\hat{C}_{8,\varepsilon}^*)^4 + (\hat{C}_{8,\varepsilon}^{**})^4 \right) \leq Ch^8 \varepsilon^{-4k_8}, \end{aligned} \quad (4.24)$$

in which the established estimates (3.25), (3.47) and (4.5) have been repeatedly applied.

To estimate the continuous inner product I_1 in (4.23), the following identity is observed:

$$(\Phi_N^{n+1})^2 + \Phi_N^{n+1}\phi_{\mathbf{F}}^{n+1} + (\phi_{\mathbf{F}}^{n+1})^2 = 3(\Phi_N^{n+1})^2 - 3\Phi_N^{n+1}e_{\mathbf{F}}^{n+1} + (e_{\mathbf{F}}^{n+1})^2. \quad (4.25)$$

This in turn gives

$$I_1 \geq 3 \left\langle (\Phi_N^{n+1})^2, (e_{\mathbf{F}}^{n+1})^2 \right\rangle + \mathcal{IE}, \quad \mathcal{IE} = -3 \left\langle \Phi_N^{n+1}e_{\mathbf{F}}^{n+1}, (e_{\mathbf{F}}^{n+1})^2 \right\rangle. \quad (4.26)$$

In terms of the additional nonlinear error inner product term, an application of Hölder inequality, combined with Sobolev inequality, indicates that

$$|\mathcal{IE}| \leq 3\|\Phi_N^{n+1}\|_{L^\infty} \cdot \|e_{\mathbf{F}}^{n+1}\|_{L^3}^3 \leq C\|\Phi_N^{n+1}\|_{H^2} \cdot \|e_{\mathbf{F}}^{n+1}\|_{L^3}^3 \leq C\hat{C}_{2,\varepsilon}^* \|e_{\mathbf{F}}^{n+1}\|_{L^3}^3, \quad (4.27)$$

with estimate (3.47) applied in the last step. To control $\|e_{\mathbf{F}}^{n+1}\|_{L^3}$, we see that

$$\begin{aligned} e_{\mathbf{F}}^{n+1} &= \hat{e}_{\mathbf{F}}^{n+1} + (e_{\mathbf{F}}^{n+1} - 2e_{\mathbf{F}}^n + e_{\mathbf{F}}^{n-1}), \quad \text{so that} \\ \|e_{\mathbf{F}}^{n+1}\|_{L^3}^3 &\leq C \left(\|\hat{e}_{\mathbf{F}}^{n+1}\|_{L^3}^3 + \|e_{\mathbf{F}}^{n+1} - 2e_{\mathbf{F}}^n + e_{\mathbf{F}}^{n-1}\|_{L^3}^3 \right) \\ &\leq C \left(\|\hat{e}_{\mathbf{F}}^{n+1}\|_{L^3}^3 + \|e_{\mathbf{F}}^{n+1} - 2e_{\mathbf{F}}^n + e_{\mathbf{F}}^{n-1}\|_{H^1}^3 \right) \leq C \left(\|\hat{e}_{\mathbf{F}}^{n+1}\|_{L^3}^3 + \Delta t^6 (\hat{Q}_{1,\varepsilon}^{**})^3 \right), \end{aligned} \quad (4.28)$$

with the preliminary estimate (4.7) applied in the last step. Meanwhile, the term $\|\hat{e}_{\mathbf{F}}^{n+1}\|_{L^3}$ could be analyzed with the help of the Sobolev inequalities:

$$\begin{aligned} \|\hat{e}_{\mathbf{F}}^{n+1}\|_{L^3} &\leq C\|\hat{e}_{\mathbf{F}}^{n+1}\|_{H^{\frac{1}{2}}} \leq C\|\hat{e}_{\mathbf{F}}^{n+1}\|_{H^{-1}}^{\frac{3}{4}} \cdot \|\hat{e}_{\mathbf{F}}^{n+1}\|_{H^5}^{\frac{1}{4}} \\ &\leq C(\hat{C}_{5,\varepsilon}^{**})^{\frac{1}{4}} \cdot \|\hat{e}_{\mathbf{F}}^{n+1}\|_{H^{-1}}^{\frac{3}{4}} \leq C(\hat{C}_{5,\varepsilon}^{**})^{\frac{1}{4}} \left(\Delta t^{\frac{15}{8}} + h^{\frac{15}{4}} \right)^{\frac{3}{4}}. \end{aligned} \quad (4.29)$$

Similarly, the preliminary estimate (4.5) has been applied in the third step and the a-priori assumption (4.21) has been recalled in the last step, since \hat{e}^{n+1} is only involved with the numerical errors at t^n and t^{n-1} . In turn, a combination of (4.28)-(4.29) and (4.27) leads to

$$|\mathcal{IE}| \leq \hat{R}_{2,\varepsilon}^* \left(\Delta t^{\frac{135}{32}} + h^{\frac{135}{16}} \right) + \hat{R}_{3,\varepsilon}^* \Delta t^6, \quad (4.30)$$

with $\hat{R}_{2,\varepsilon}^* = C\hat{C}_{2,\varepsilon}^* (\hat{C}_{5,\varepsilon}^{**})^{\frac{3}{4}}$, $\hat{R}_{3,\varepsilon}^* = C\hat{C}_{2,\varepsilon}^* (\hat{Q}_{1,\varepsilon}^{**})^3$. Going back (4.26), we get

$$I_1 \geq 3 \left((\Phi_N^{n+1})^2, (e_{\mathbf{F}}^{n+1})^2 \right) - \hat{R}_{2,\varepsilon}^* \left(\Delta t^{\frac{135}{32}} + h^{\frac{135}{16}} \right) - \hat{R}_{3,\varepsilon}^* \Delta t^6. \quad (4.31)$$

Therefore, a substitution of (4.10), (4.11), (4.16), (4.17), (4.20), (4.22), (4.24) and (4.31) into (4.9) yields

$$\begin{aligned} & \frac{1}{2\Delta t} \left(\|e^{n+1}\|_{-1,h}^2 - \|e^n\|_{-1,h}^2 + \|2e^{n+1} - e^n\|_{-1,h}^2 - \|2e^n - e^{n-1}\|_{-1,h}^2 \right) \\ & + A\varepsilon^{-1} \Delta t \left(\|\nabla_{h,(4)} e^{n+1}\|_2^2 - \|\nabla_{h,(4)} e^n\|_2^2 \right) + 2 \left(\varepsilon^{-1} \left(3(\Phi_N^{n+1})^2 - 1, (e_{\mathbf{F}}^{n+1})^2 \right) + \varepsilon \|\nabla e_{\mathbf{F}}^{n+1}\|_2^2 \right) \\ & \leq \|\tau^{n+1}\|_{-1,h}^2 + \|e^{n+1}\|_{-1,h}^2 + \|e_{\mathbf{F}}^{n+1}\|_{H^{-1}}^2 + C(\varepsilon(\hat{C}_{7,\varepsilon}^{**})^2 + \varepsilon^{-4k_8})h^8 \\ & + \varepsilon^{-2}(\hat{Q}_{1,\varepsilon}^{**})^2 \Delta t^4 + 2\varepsilon^{-1} \left(\hat{R}_{2,\varepsilon}^* \left(\Delta t^{\frac{135}{32}} + h^{\frac{135}{16}} \right) + \hat{R}_{3,\varepsilon}^* \Delta t^6 \right). \end{aligned} \quad (4.32)$$

On the other hand, a careful application of the linearized spectrum estimate (4.8) (reviewed in Proposition 4.2, by [22]) reveals that

$$\varepsilon^{-1} \left(3(\Phi_N^{n+1})^2 - 1, (e_{\mathbf{F}}^{n+1})^2 \right) + \varepsilon \|\nabla e_{\mathbf{F}}^{n+1}\|_2^2 \geq -C_0 \|e_{\mathbf{F}}^{n+1}\|_{H^{-1}}^2 \geq -C_0 \|e^{n+1}\|_{-1,h}^2, \quad (4.33)$$

in which inequality (2.18) (in Lemma 2.3) has been applied at the last step. Subsequently, with an introduction of error norm quantity

$$E^n := \frac{1}{2} (\|e^n\|_{-1,h}^2 + \|2e^n - e^{n-1}\|_{-1,h}^2) + A\varepsilon^{-1} \Delta t^2 \|\nabla_{h,(4)} e^n\|_2^2, \quad (4.34)$$

we obtain

$$\begin{aligned} \frac{1}{\Delta t} (E^{n+1} - E^n) & \leq \|\tau^{n+1}\|_{-1,h}^2 + (2C_0 + 1) \|e^{n+1}\|_{-1,h}^2 + \|e_{\mathbf{F}}^{n+1}\|_{H^{-1}}^2 + C(\varepsilon(\hat{C}_{7,\varepsilon}^{**})^2 + \varepsilon^{-4k_8})h^8 \\ & + \varepsilon^{-2}(\hat{Q}_{1,\varepsilon}^{**})^2 \Delta t^4 + 2\varepsilon^{-1} \left(\hat{R}_{2,\varepsilon}^* \left(\Delta t^{\frac{135}{32}} + h^{\frac{135}{16}} \right) + \hat{R}_{3,\varepsilon}^* \Delta t^6 \right) \\ & \leq (2C_0 + 2) \|e^{n+1}\|_{-1,h}^2 + C(\Delta t^4 + h^8) \varepsilon^{-2j_4} + C(\varepsilon(\hat{C}_{7,\varepsilon}^{**})^2 + \varepsilon^{-4k_8})h^8 \\ & + \varepsilon^{-2}(\hat{Q}_{1,\varepsilon}^{**})^2 \Delta t^4 + 2\varepsilon^{-1} \left(\hat{R}_{2,\varepsilon}^* \left(\Delta t^{\frac{135}{32}} + h^{\frac{135}{16}} \right) + \hat{R}_{3,\varepsilon}^* \Delta t^6 \right) \\ & \leq (4C_0 + 4) E^{n+1} + C(\Delta t^4 + h^8) (\varepsilon^{-2j_4} + \varepsilon(\hat{C}_{7,\varepsilon}^{**})^2 + \varepsilon^{-4k_8} + \varepsilon^{-2}(\hat{Q}_{1,\varepsilon}^{**})^2) \\ & + 2\varepsilon^{-1} \left(\hat{R}_{2,\varepsilon}^* \left(\Delta t^{\frac{135}{32}} + h^{\frac{135}{16}} \right) + \hat{R}_{3,\varepsilon}^* \Delta t^6 \right), \end{aligned} \quad (4.35)$$

in which inequality (2.18) was applied in the second step, and the third step comes from the fact that $\|e^{n+1}\|_{-1,h}^2 \leq 2E^{n+1}$. In addition, under the following constraint for the time step and space mesh size:

$$\begin{aligned} \hat{R}_{2,\varepsilon}^* \varepsilon^{-1} \Delta t^{\frac{7}{32}} & \leq \frac{1}{4}, \quad \hat{R}_{2,\varepsilon}^* \varepsilon^{-1} h^{\frac{7}{16}} \leq \frac{1}{2}, \quad \hat{R}_{3,\varepsilon}^* \varepsilon^{-1} \Delta t^2 \leq \frac{1}{4}, \\ \text{i.e. } \Delta t, h & \leq \min \left(\left(\frac{\varepsilon}{4} (\hat{R}_{2,\varepsilon}^*)^{-1} \right)^{\frac{32}{7}}, \left(\frac{\varepsilon}{4} (\hat{R}_{3,\varepsilon}^*)^{-1} \right)^{\frac{1}{2}} \right), \end{aligned} \quad (4.36)$$

the following inequality is valid:

$$\begin{aligned} \frac{1}{\Delta t}(E^{n+1} - E^n) &\leq (4C_0 + 4)E^{n+1} + \hat{R}_{4,\varepsilon}^*(\Delta t^4 + h^8), \\ \hat{R}_{4,\varepsilon}^* &= C(\varepsilon^{-2j_4} + \varepsilon(\hat{C}_{7,\varepsilon}^{**})^2 + \varepsilon^{-4k_8} + \varepsilon^{-2}(\hat{Q}_{1,\varepsilon}^{**})^2) + 1. \end{aligned} \quad (4.37)$$

Of course, $4C_0 + 4$ is a constant independent on ε , and $\hat{R}_{4,\varepsilon}^*$ depends on ε^{-1} in a polynomial form. In turn, an application of discrete Gronwall inequality to (4.37) gives the desired error estimate:

$$\|e^{n+1}\|_{-1,h}^2 \leq 2E^{n+1} \leq C_2 e^{(4C_0+5)T} \hat{R}_{4,\varepsilon}^*(\Delta t^4 + h^8). \quad (4.38)$$

Recovery of the a-priori assumption (4.21) With the convergence estimate (4.38) at hand, it is obvious that the a-priori assumption (4.21) could be recovered at the next time step, t^{n+1} , under the following constraint for Δt and h :

$$\begin{aligned} C_2 e^{(4C_0+5)T} \hat{R}_{4,\varepsilon}^* \max(\Delta t^{\frac{1}{4}}, h^{\frac{1}{2}}) &\leq 1, \\ \text{i.e. } \Delta t &\leq (C_2 e^{(4C_0+5)T} \hat{R}_{4,\varepsilon}^*)^{-4}, \quad h \leq (C_2 e^{(4C_0+5)T} \hat{R}_{4,\varepsilon}^*)^{-2}. \end{aligned} \quad (4.39)$$

In turn, we can take $C_0^* = 2C_0 + \frac{5}{2}$, $\hat{R}^* = C_2^{\frac{1}{2}} e^{(2C_0+\frac{5}{2})T} (\hat{R}_{4,\varepsilon}^*)^{\frac{1}{2}}$. This matches the form of (2.43), in which the integer index J_0 could be chosen according to the form of $\hat{R}_{4,\varepsilon}^*$.

Moreover, based on the dependence of $\hat{R}_{2,\varepsilon}^*$, $\hat{R}_{4,\varepsilon}^*$ in terms of ε^{-1} , the values of J_1 and J_2 could be appropriately taken. In other words, the constraints (4.36) and (4.39) for Δt and h could be converted into the form of (2.42). As a result, the proof of Theorem 2.8 is finished.

Remark 4.3. *A refined error estimate has been reported for a Crank-Nicolson-style, energy stable semi-discrete numerical scheme [28], while the space was kept continuous. For the fully discrete Crank-Nicolson-style numerical schemes [16, 17, 27], with either finite difference, mixed finite element or Fourier pseudo-spectral spatial approximation, the analysis could be naturally extended, following similar ideas of this article. Of course, for the BDF-style, energy stable numerical schemes, with other choices of spatial discretization, the refined error analysis (with an improved convergence constant) could also be similarly derived. The technical details are expected to be very involved and are left to interested readers.*

The refined error estimate for the third and even higher order (in time) numerical schemes for the Allen-Cahn/Cahn-Hilliard equation, such as [11, 15], will be considered in the future works.

5 The numerical results

In this section we provide a numerical accuracy check for the proposed numerical scheme (2.31). The computational domain is set as $\Omega = (0, 3.2)^3$, and the exact profile for the phase variable is chosen to be

$$\Phi(x, y, t) = \cos\left(\frac{5}{8}\pi x\right) \sin\left(\frac{5}{8}\pi y\right) \cos\left(\frac{5}{8}\pi z\right) \cos(t). \quad (5.1)$$

Of course, we need to add an artificial, time-dependent forcing term to make this exact profile satisfy the original equation (1.2). Based on this PDE with a forced term, the proposed fourth order difference scheme (2.31) is implemented, using the multi-grid approach. Such an iteration solver has been outlined in [27] for a second order difference scheme, while its extension to the fourth order finite difference approximation is straightforward.

In the accuracy check, we set the time step size as $\Delta t = h^2$, with $h = \frac{L}{N}$ ($L = 3.2$), so that the second order temporal accuracy corresponds to the fourth order spatial accuracy. The final time set

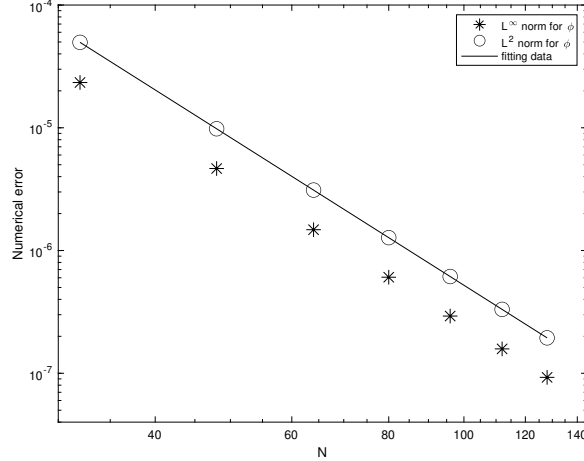


Figure 1: The discrete ℓ^2 and ℓ^∞ numerical errors versus spatial resolution N for $N = 32 : 16 : 128$, and the time step size is set as $\Delta t = h^2$. The numerical results are obtained by the computation using the proposed numerical scheme (2.31). The surface diffusion parameter is taken to be $\varepsilon = 1$. The data lie roughly on curves CN^{-4} for appropriate choices of C , confirming the full fourth order spatial accuracy and second order temporal accuracy.

by $T = 0.16$, and the surface diffusion parameter is given by $\varepsilon = 1$. A sequence of spatial resolutions are taken as $N = 32 : 16 : 128$. The expected numerical accuracy assumption $e = C(\Delta t^2 + h^4)$ indicates that $\ln |e| = \ln C - 4 \ln N$. In turn, we plot $\ln |e|$ versus $\ln N$ to demonstrate the temporal convergence order. The fitted line displayed in Figure 1 shows an approximate slope of -3.9905 , which confirms almost a perfect fourth order convergence in space.

This accuracy check confirms the local-in-time convergence property of the fourth order finite difference numerical scheme (2.31). In terms of the long time behavior of this numerical scheme, the two-dimensional simulation results of the coarsening process has been presented in [12], in a square domain $\Omega = (0, 12.8)^2$, with a surface diffusion coefficient $\varepsilon = 0.03$. An almost perfect $t^{-1/3}$ energy dissipation law has been reported in the long time simulation, which in turn verifies the theoretical analysis provided in this article.

6 Concluding remarks

A refined error analysis is presented for a modified BDF2 in time, fourth order long stencil finite difference numerical scheme to the 3-D Cahn-Hilliard equation. The Fourier analysis has to be applied to analyze the functional norms associated with the fourth order long stencil spatial approximation, and the difference between the discrete and continuous inner product has to be estimated in an accurate way. For the fully discrete numerical scheme, a uniform-in-time H^m bound of the numerical solution, for any $m \geq 2$, as well as the associated H^k bounds for the first and second order temporal difference stencil, namely $\|\phi_{\mathbf{F}}^{n+1} - \phi_{\mathbf{F}}^n\|_{H^k}$ and $\|\phi_{\mathbf{F}}^{n+1} - 2\phi_{\mathbf{F}}^n + \phi_{\mathbf{F}}^{n-1}\|_{H^k}$, are needed to obtain a refined convergence constant. All these functional bounds have to be carefully derived through Sobolev estimates in the fourth order finite difference space. Certain recursive analysis has been applied in the analysis for the BDF2 temporal stencil. In the error estimate, we have to apply a spectrum estimate for the linearized Cahn-Hilliard operator, so that all the numerical error inner product terms, in the discrete H^{-1} space, are analyzed in a unified way. Using this analytic

approach, an application of the discrete Gronwall inequality avoids a convergence constant of the form $\exp(CT\varepsilon^{-m})$; instead, the constant turns out to be dependent on ε^{-1} only in a polynomial order. A three-dimensional numerical example of accuracy check is also presented, which confirms the theoretical analysis in this article.

7 Acknowledgments

This work is supported in part by the NSF DMS-2012269, DMS-2309548 (C. Wang), NSFC 12001358 (Y. Yan), and NSFC 11971342, 12371401 (X. Yue).

A Proof of Lemma 2.3

Proof. For the discrete grid function f and its continuous extension $f_{\mathbf{F}}$, given by (2.11) and (2.12), Parseval's identity (at both the discrete and continuous levels) implies that

$$\|f\|_2^2 = \|f_{\mathbf{F}}\|_{L^2}^2 = L^3 \sum_{\ell, m, n=-K}^K |\hat{f}_{\ell, m, n}^N|^2, \quad \text{since } hN = L. \quad (\text{A.1})$$

For the comparison between the discrete and continuous gradient and Laplacian operators, we start with the following Fourier expansions:

$$(D_x f)_{i+1/2, j, k} = \sum_{\ell, m, n=-K}^K \mu_{\ell} \hat{f}_{\ell, m, n}^N e^{2\pi i(\ell x_{i+1/2} + m y_j + n z_k)/L}, \quad (\text{A.2})$$

$$(D_x^2 f)_{i, j, k} = \sum_{\ell, m, n=-K}^K -|\mu_{\ell}|^2 \hat{f}_{\ell, m, n}^N e^{2\pi i(\ell x_{i+1/2} + m y_j + n z_k)/L}, \quad (\text{A.3})$$

$$\partial_x f_{\mathbf{F}}(x, y, z) = \sum_{\ell, m, n=-K}^K \nu_{\ell} \hat{f}_{\ell, m, n}^N e^{2\pi i(\ell x + m y + n z)/L}, \quad (\text{A.4})$$

$$\text{with } \mu_{\ell} = -\frac{2i \sin \frac{\ell \pi h}{L}}{h}, \quad \nu_{\ell} = -\frac{2i \ell \pi}{L}. \quad (\text{A.5})$$

In turn, an application of Parseval's identity yields

$$\|D_x f\|_2^2 = L^3 \sum_{\ell, m, n=-K}^K |\mu_{\ell}|^2 |\hat{f}_{\ell, m, n}^N|^2, \quad \|\partial_x f_{\mathbf{F}}\|_{L^2}^2 = L^3 \sum_{\ell, m, n=-K}^K |\nu_{\ell}|^2 |\hat{f}_{\ell, m, n}^N|^2. \quad (\text{A.6})$$

The comparison of Fourier eigenvalues between $|\mu_{\ell}|$ and $|\nu_{\ell}|$ shows that

$$\frac{2}{\pi} |\nu_{\ell}| \leq |\mu_{\ell}| \leq |\nu_{\ell}|, \quad \text{for } -K \leq \ell \leq K. \quad (\text{A.7})$$

This indicates that

$$\frac{2}{\pi} \|\partial_x \phi_{\mathbf{F}}\|_{L^2} \leq \|D_x \phi\|_2 \leq \|\partial_x \phi_{\mathbf{F}}\|_{L^2}. \quad (\text{A.8})$$

Similar comparison estimates can be derived in the same manner to reveal that

$$\frac{2}{\pi} \|\nabla \phi_{\mathbf{F}}\|_{L^2} \leq \|\nabla_h \phi\|_2 \leq \|\nabla \phi_{\mathbf{F}}\|_{L^2}. \quad (\text{A.9})$$

This gives (2.17) in Lemma 2.3, with $j = 0$. It can be proved analogously that

$$(2\pi^{-1})^{2j} \|\Delta^j \phi_{\mathbf{F}}\|_{L^2} \leq \|\Delta_h^j \phi\|_2 \leq \|\Delta^j \phi_{\mathbf{F}}\|_{L^2}, \quad (\text{A.10})$$

$$(2\pi^{-1})^{2j+1} \|\nabla \Delta^j \phi_{\mathbf{F}}\|_{L^2} \leq \|\nabla_h \Delta_h^j \phi\|_2 \leq \|\nabla \Delta^j \phi_{\mathbf{F}}\|_{L^2}, \quad (\text{A.11})$$

for any $j \geq 1$. As a result, both (2.16) and (2.17) have been established.

In turn, estimate (2.19) is a direct consequence of (A.10)-(A.11), combined with the preliminary inequality (2.10) (in Lemma 2.1), as well as the elliptic regularity at the continuous level:

$$\begin{aligned} \|\Delta_{h,(4)} f\|_2 &\leq \frac{4}{3} \|\Delta_h f\|_2 \leq \frac{4}{3} \|\Delta f_{\mathbf{F}}\| \leq \frac{4}{3} C_1^* \|\Delta^2 f_{\mathbf{F}}\| \\ &\leq \frac{4}{3} C_1^* (D_4)^{-1} \|\Delta_h^2 f\|_2 \leq \frac{4}{3} C_1^* (D_4)^{-1} \|\Delta_{h,(4)}^2 f\|_2, \end{aligned} \quad (\text{A.12})$$

in which C_1^* is denoted as the elliptic regularity constant at the continuous level. Therefore, (2.19) has been proven, by taking $C_1 = \frac{4}{3} C_1^* (D_4)^{-1}$.

To prove (2.18), we first observe that $\int_{\Omega} f_{\mathbf{F}} d\mathbf{x} = |\Omega| \cdot \bar{f} = 0$, since $f_{\mathbf{F}} = 0$. In turn, a careful calculation reveals the discrete Fourier expansion for $(-\Delta_{h,(4)})^{-1} f$ and the continuous Fourier expansion for $(-\Delta)^{-1} f_{\mathbf{F}}$

$$(-\Delta_{h,(4)})^{-1} f_{i,j,k} = \sum_{\ell,m,n=-K, (\ell,m,n) \neq \mathbf{0}}^K (\lambda_{\ell,m,n}^{(4)})^{-1} \hat{f}_{\ell,m,n}^N e^{2\pi i(\ell x_i + m y_j + n z_k)/L}, \quad (\text{A.13})$$

$$(-\Delta)^{-1} f_{\mathbf{F}}(x, y, z) = \sum_{\ell,m,n=-K, (\ell,m,n) \neq \mathbf{0}}^K \Lambda_{\ell,m,n}^{-1} \hat{f}_{\ell,m,n}^N e^{2\pi i(\ell x + m y + n z)/L}, \quad (\text{A.14})$$

$$\text{with } \lambda_{\ell,m,n}^{(4)} = \lambda_{\ell}^{(4)} + \lambda_m^{(4)} + \lambda_n^{(4)}, \quad \lambda_k^{(4)} = \lambda_k + \frac{h^2}{12} \lambda_k^2, \quad \lambda_k = \frac{4 \sin^2 \frac{k\pi h}{L}}{h^2}, \quad (0 \leq k \leq K), \quad (\text{A.15})$$

$$\Lambda_{\ell,m,n} = \Lambda_{\ell} + \Lambda_m + \Lambda_n, \quad \Lambda_k = \frac{4k^2 \pi^2}{L^2}, \quad (0 \leq k \leq K). \quad (\text{A.16})$$

with the zero vector defined as $\mathbf{0} = (0, 0, 0)$. Furthermore, an application of the Parseval equality to the discrete Fourier expansion for $\nabla_{h,(4)}((-\Delta_{h,(4)})^{-1} f)$ and the continuous Fourier expansion for $\nabla((-\Delta)^{-1} f_{\mathbf{F}})$ implies that

$$\|f\|_{-1,h}^2 = \|\nabla_{h,(4)}(-\Delta_{h,(4)})^{-1} f\|_2^2 = L^3 \sum_{\ell,m,n=-K, (\ell,m,n) \neq \mathbf{0}}^K (\lambda_{\ell,m,n}^{(4)})^{-1} \left| \hat{f}_{\ell,m,n}^N \right|^2, \quad (\text{A.17})$$

$$\begin{aligned} \|f_{\mathbf{F}}\|_{H^{-1}}^2 &= \|\nabla(-\Delta)^{-1} f_{\mathbf{F}}\|_2^2 = L^3 \sum_{\ell,m,n=-K, (\ell,m,n) \neq \mathbf{0}}^K \Lambda_{\ell,m,n}^{-2} (|\nu_{\ell}|^2 + |\nu_m|^2 + |\nu_n|^2) \left| \hat{f}_{\ell,m,n}^N \right|^2 \\ &= L^3 \sum_{\ell,m,n=-K, (\ell,m,n) \neq \mathbf{0}}^K \Lambda_{\ell,m,n}^{-1} \left| \hat{f}_{\ell,m,n}^N \right|^2, \end{aligned} \quad (\text{A.18})$$

based on the following fact

$$|\nu_{\ell}|^2 + |\nu_m|^2 + |\nu_n|^2 = \Lambda_{\ell,m,n}. \quad (\text{A.19})$$

Meanwhile, the eigenvalue comparison estimate (A.7) indicates that

$$\frac{4}{\pi^2} \Lambda_{\ell,m,n} \leq \lambda_{\ell,m,n}^{(4)} \leq \Lambda_{\ell,m,n}, \quad \forall -K \leq \ell, m, n \leq K. \quad (\text{A.20})$$

Its combination with (A.17) and (A.18) yields

$$\|f_{\mathbf{F}}\|_{H^{-1}}^2 \leq \|f\|_{-1,h}^2 \leq \frac{\pi^2}{4} \|f_{\mathbf{F}}\|_{H^{-1}}^2. \quad (\text{A.21})$$

Therefore, (2.18) has been proven, by taking $D_{-1} = \frac{\pi}{2}$.

Similar techniques can be used to establish (2.20). We have the discrete Fourier expansion for $\Delta_{h,(4)}f$ and the continuous Fourier expansion for $\Delta f_{\mathbf{F}}$

$$\Delta_{h,(4)}f_{i,j,k} = - \sum_{\ell,m,n=-K}^K \lambda_{\ell,m,n}^{(4)} \hat{f}_{\ell,m,n}^N e^{2\pi i(\ell x_i + m y_j + n z_k)/L}, \quad \text{so that} \quad (\text{A.22})$$

$$(\Delta_{h,(4)}f)_{\mathbf{F}}(x, y, z) = - \sum_{\ell,m,n=-K}^K \lambda_{\ell,m,n}^{(4)} \hat{f}_{\ell,m,n}^N e^{2\pi i(\ell x + m y + n z)/L}, \quad (\text{A.23})$$

$$\Delta f_{\mathbf{F}}(x, y, z) = - \sum_{\ell,m,n=-K}^K \Lambda_{\ell,m,n} \hat{f}_{\ell,m,n}^N e^{2\pi i(\ell x + m y + n z)/L}. \quad (\text{A.24})$$

Estimate (2.20), with $m = 0$, is a direct consequence of the eigenvalue comparison estimate (A.20). To make a comparison between their H^m norm, we observe the following Fourier expansion of their corresponding ∂_x derivatives:

$$\partial_x(\Delta_{h,(4)}f)_{\mathbf{F}}(x, y, z) = - \sum_{\ell,m,n=-K}^K \nu_{\ell} \lambda_{\ell,m,n}^{(4)} \hat{f}_{\ell,m,n}^N e^{2\pi i(\ell x + m y + n z)/L}, \quad (\text{A.25})$$

$$\partial_x \Delta f_{\mathbf{F}}(x, y, z) = - \sum_{\ell,m,n=-K}^K \nu_{\ell} \Lambda_{\ell,m,n} \hat{f}_{\ell,m,n}^N e^{2\pi i(\ell x + m y + n z)/L}, \quad (\text{A.26})$$

and an application of Parseval equality implies that

$$\|\partial_x(\Delta_h f)_{\mathbf{F}}\|^2 = L^3 \sum_{\ell,m,n=-K}^K |\nu_{\ell}|^2 (\lambda_{\ell,m,n}^{(4)})^2 \left| \hat{f}_{\ell,m,n}^N \right|^2, \quad (\text{A.27})$$

$$\|\partial_x \Delta f_{\mathbf{F}}\|^2 = L^3 \sum_{\ell,m,n=-K}^K |\nu_{\ell}|^2 \Lambda_{\ell,m,n}^2 \left| \hat{f}_{\ell,m,n}^N \right|^2. \quad (\text{A.28})$$

By the estimate eigenvalue comparison estimate (A.20), we conclude that

$$\|\partial_x(\Delta_h f)_{\mathbf{F}}\|^2 \leq \|\partial_x \Delta f_{\mathbf{F}}\|^2. \quad (\text{A.29})$$

Similar estimates can be derived for other partial derivatives, and higher order derivatives. Therefore, (2.20) is valid for any $m \geq 0$. The proof of Lemma 2.3 is complete. \square

B Proof of Lemma 2.4

Proof. Based on the Fourier expansions (A.2)-(A.5), we apply the Parseval equality and get

$$\|D_x f\|_2^2 = L^3 \sum_{\ell, m, n=-K}^K |\mu_\ell|^2 \cdot \left| \hat{f}_{\ell, m, n}^N \right|^2, \quad \|D_x^2 f\|_2^2 = L^3 \sum_{\ell, m, n=-K}^K |\mu_\ell|^4 \cdot \left| \hat{f}_{\ell, m, n}^N \right|^2 \quad (\text{B.1})$$

$$\|\partial_x f_{\mathbf{F}}\|_2^2 = L^3 \sum_{\ell, m, n=-K}^K |\nu_\ell|^2 \cdot \left| \hat{f}_{\ell, m, n}^N \right|^2, \quad (\text{B.2})$$

$$\text{so that } \|\partial_x f_{\mathbf{F}}\|_2^2 - \|\mathcal{D}_{x,(4)} f\|_2^2 = L^3 \sum_{\ell, m, n=-K}^K \left(|\nu_\ell|^2 - (|\mu_\ell|^2 + \frac{h^2}{12} |\mu_\ell|^4) \right) \left| \hat{f}_{\ell, m, n}^N \right|^2. \quad (\text{B.3})$$

Furthermore, the following estimates are available:

$$\sin \frac{\ell\pi h}{L} = \frac{\ell\pi h}{L} - \frac{1}{6} \left(\frac{\ell\pi h}{L} \right)^3 - \frac{\cos \eta}{120} \left(\frac{\ell\pi h}{L} \right)^5, \quad \eta \in (0, \frac{\pi}{2}), \quad (\text{B.4})$$

$$\sin^2 \left(\frac{\ell\pi h}{L} \right) = \left(\frac{\ell\pi h}{L} \right)^2 - \frac{1}{3} \left(\frac{\ell\pi h}{L} \right)^4 + \left(\frac{1}{36} + \frac{\cos \eta}{60} \right) \left(\frac{\ell\pi h}{L} \right)^6 + \xi_1 \left(\frac{\ell\pi h}{L} \right)^8, \quad |\xi_1| \leq \frac{1}{360}, \quad (\text{B.5})$$

$$1 + \frac{h^2}{12} |\mu_\ell|^2 = 1 + \frac{1}{3} \sin^2 \left(\frac{\ell\pi h}{L} \right) = 1 + \frac{1}{3} \left(\frac{\ell\pi h}{L} \right)^2 + \xi_2 \left(\frac{\ell\pi h}{L} \right)^4, \quad -\frac{1}{9} \leq \xi_2 \leq -\frac{1}{12}, \quad (\text{B.6})$$

$$\begin{aligned} \text{so that } 0 \leq |\nu_\ell|^2 - |\mu_\ell|^2 (1 + \frac{h^2}{12} |\mu_\ell|^2) &= \left(\frac{1}{3} - \frac{\cos \eta}{15} - 4\xi_2 \right) h^4 \left(\frac{\ell\pi}{L} \right)^6 + \xi_3 h^6 \left(\frac{\ell\pi}{L} \right)^8 \quad \left(-\frac{2}{9} \leq \xi_3 \leq 0 \right) \\ &\leq h^4 \left(\frac{\ell\pi}{L} \right)^6 = \frac{1}{64} h^4 \left(\frac{2\ell\pi}{L} \right)^6, \end{aligned} \quad (\text{B.7})$$

in which the eigenvalue representation formula (A.5) was recalled, and a Taylor expansion was performed in (B.4). Going back (B.3), we arrive at

$$0 \leq \|\partial_x f_{\mathbf{F}}\|_2^2 - \|\mathcal{D}_{x,(4)} f\|_2^2 \leq \frac{L^3}{64} \sum_{\ell, m, n=-K}^K h^4 \left(\frac{2\ell\pi}{L} \right)^6 \left| \hat{f}_{\ell, m, n}^N \right|^2 = \frac{h^4}{64} \|\partial_x^3 f_{\mathbf{F}}\|_2^2. \quad (\text{B.8})$$

Two other estimates could be derived in a similar way:

$$0 \leq \|\partial_y f_{\mathbf{F}}\|_2^2 - \|\mathcal{D}_{y,(4)} f\|_2^2 \leq \frac{h^4}{64} \|\partial_y^3 f_{\mathbf{F}}\|_2^2, \quad 0 \leq \|\partial_z f_{\mathbf{F}}\|_2^2 - \|\mathcal{D}_{z,(4)} f\|_2^2 \leq \frac{h^4}{64} \|\partial_z^3 f_{\mathbf{F}}\|_2^2. \quad (\text{B.9})$$

A combination of (B.8) and (B.9) results in

$$0 \leq \|\nabla f_{\mathbf{F}}\|_2^2 - \|\nabla_{h,(4)} f\|_2^2 \leq \frac{h^4}{64} \|f_{\mathbf{F}}\|_{H^3}^2. \quad (\text{B.10})$$

The proof of Lemma 2.4 is complete. \square

C Proof of Lemma 2.5

Proof. (1) In addition to (2.11) and (2.12), we set the discrete Fourier expansion for g and its continuous extension given by

$$g_{i,j,k} = \sum_{\ell,m,n=-K}^K \hat{g}_{\ell,m,n}^N e^{2\pi i(\ell x_i + m y_j + n z_k)/L}, \quad (\text{C.1})$$

$$\mathbf{g}(x, y, z) = g_{\mathbf{F}}(x, y, z) = \sum_{\ell,m,n=-K}^K \hat{g}_{\ell,m,n}^N e^{2\pi i(\ell x + m y + n z)/L}. \quad (\text{C.2})$$

In turn, we assume the Fourier expansion for the product function $\mathbf{f} \cdot \mathbf{g}$ as

$$(\mathbf{f} \cdot \mathbf{g})(x, y, z) = \sum_{\ell,m,n=-2K}^{2K} \hat{h}_{\ell,m,n}^N e^{2\pi i(\ell x + m y + n z)/L}. \quad (\text{C.3})$$

In particular, it is observed that $\mathbf{f} \cdot \mathbf{g} \in \mathcal{B}^{2K}$. Consequently, the discrete product function $f \cdot g$ turns out to be the projection of $\mathbf{f} \cdot \mathbf{g}$ at the numerical grid points:

$$(f \cdot g)_{i,j,k} = (\mathbf{f} \cdot \mathbf{g})(x_i, j_j, z_k) = \mathcal{I}_N(\mathbf{f} \cdot \mathbf{g})(x_i, j_j, z_k). \quad (\text{C.4})$$

A more careful expansion shows that

$$\overline{f \cdot g} = \frac{1}{|\Omega|} \int_{\Omega} \mathcal{I}_N(\mathbf{f} \cdot \mathbf{g}) d\mathbf{x} = \frac{1}{|\Omega|} \int_{\Omega} \mathbf{f} \cdot \mathbf{g} d\mathbf{x}, \quad (\text{C.5})$$

which is equivalent to (2.29). In more detail, the first step comes from the fact that $\mathcal{I}_N \mathbf{f} \cdot \mathbf{g} \in \mathcal{B}^K$, and the second step is based on the fact that, there is no aliasing error on the mode of $(\ell, m, n) = \mathbf{0}$, between $\mathbf{f} \cdot \mathbf{g} \in \mathcal{B}^{2K}$ and its projection onto \mathcal{B}^K .

(2) In the general case, we note that f and g are discrete interpolations of $\mathcal{I}_N \mathbf{f} \in \mathcal{B}^K$ and $\mathcal{I}_N \mathbf{g} \in \mathcal{B}^K$. By (2.29), we arrive at

$$\begin{aligned} |\langle f, g \rangle - (\mathbf{f}, \mathbf{g})| &= |(\mathcal{I}_N \mathbf{f}, \mathcal{I}_N \mathbf{g}) - (\mathbf{f}, \mathbf{g})| \leq |(\mathcal{I}_N \mathbf{f} - \mathbf{f}, \mathcal{I}_N \mathbf{g})| + |(\mathbf{f}, \mathcal{I}_N \mathbf{g} - \mathbf{g})| \\ &\leq \|\mathcal{I}_N \mathbf{f} - \mathbf{f}\| \cdot \|\mathcal{I}_N \mathbf{g}\| + \|\mathbf{f}\| \cdot \|\mathcal{I}_N \mathbf{g} - \mathbf{g}\| \\ &\leq Ch^8 (\|\mathbf{f}\|_{H^8} \cdot \|\mathbf{g}\|_{H^2} + \|\mathbf{f}\|_{H^2} \cdot \|\mathbf{g}\|_{H^8}), \end{aligned} \quad (\text{C.6})$$

which gives (2.30), with the Fourier spectral interpolation approximation (2.25) applied at the last step. The proof of Lemma 2.5 is complete. \square

References

- [1] N. Alikakos, P. Bates, and X. Chen. Convergence of the Cahn-Hilliard equation to the Hele-Shaw model. *Arch. Rational Mech. Anal.*, 128 (2):165–205, 1994.
- [2] N. Alikakos and G. Fusco. The spectrum of the Cahn-Hilliard operator for generic interface in higher space dimensions. *Indiana Univ. Math. J.*, 42 (2):637–674, 1993.
- [3] J.P. Boyd. *Chebyshev and Fourier spectral methods*. Courier Corporation, 2001.

- [4] J.W. Cahn and J.E. Hilliard. Free energy of a nonuniform system. i. interfacial free energy. *J. Chem. Phys.*, 28:258–267, 1958.
- [5] C. Canuto and A. Quarteroni. Approximation results for orthogonal polynomials in Sobolev spaces. *Math. Comp.*, 38:67–86, 1982.
- [6] W. Chen, S. Conde, C. Wang, X. Wang, and S.M. Wise. A linear energy stable scheme for a thin film model without slope selection. *J. Sci. Comput.*, 52:546–562, 2012.
- [7] W. Chen, X. Wang, Y. Yan, and Z. Zhang. A second order BDF numerical scheme with variable steps for the Cahn-Hilliard equation. *SIAM J. Numer. Anal.*, 57(1):495–525, 2019.
- [8] X. Chen. Spectrum for the Allen-Cahn Cahn-Hilliard and phase-field equations for generic interfaces. *Comm. Partial Diff. Eqs.*, 19:1371–1395, 1994.
- [9] X. Chen. Global asymptotic limit of solutions of the Cahn-Hilliard equation. *J. Diff. Geom.*, 44 (2):262–311, 1996.
- [10] X. Chen, C. M. Elliott, A. Gardiner, and J. Zhao. Convergence of numerical solutions to the Allen-Cahn equation. *Appl. Anal.*, 69 (1):47–56, 1998.
- [11] X.W. Chen, X. Qian, and S. Song. Fourth-order structure-preserving method for the conservative Allen-Cahn equation. *Adv. Appl. Math. Mech.*, 15(1):159–181, 2022.
- [12] K. Cheng, W. Feng, C. Wang, and S.M. Wise. An energy stable fourth order finite difference scheme for the Cahn-Hilliard equation. *J. Comput. Appl. Math.*, 362:574–595, 2019.
- [13] K. Cheng, Z. Qiao, and C. Wang. A third order exponential time differencing numerical scheme for no-slope-selection epitaxial thin film model with energy stability. *J. Sci. Comput.*, 81(1):154–185, 2019.
- [14] K. Cheng, C. Wang, and S.M. Wise. An energy stable fourier pseudo-spectral numerical scheme for the square phase field crystal equation. *Commun. Comput. Phys.*, 26:1335–1364, 2019.
- [15] K. Cheng, C. Wang, S.M. Wise, and Y. Wu. A third order accurate in time, BDF-type energy stable scheme for the Cahn-Hilliard equation. *Numer. Math. Theor. Meth. Appl.*, 15(2):279–303, 2022.
- [16] K. Cheng, C. Wang, S.M. Wise, and X. Yue. A second-order, weakly energy-stable pseudo-spectral scheme for the Cahn-Hilliard equation and its solution by the homogeneous linear iteration method. *J. Sci. Comput.*, 69:1083–1114, 2016.
- [17] A. Diegel, C. Wang, and S.M. Wise. Stability and convergence of a second order mixed finite element method for the Cahn-Hilliard equation. *IMA J. Numer. Anal.*, 36:1867–1897, 2016.
- [18] A. Fathy, C. Wang, J. Wilson, and S. Yang. A fourth order difference scheme for the maxwell equations on yee grid. *J. Hyperbol. Differ. Eq.*, 5(03):613–642, 2008.
- [19] W. Feng, C. Wang, S.M. Wise, and Z. Zhang. A second-order energy stable Backward Differentiation Formula method for the epitaxial thin film equation with slope selection. *Numer. Methods Partial Differ. Equ.*, 34(6):1975–2007, 2018.
- [20] X. Feng and Y. Li. Analysis of interior penalty discontinuous Galerkin methods for the Allen-Cahn equation and the mean curvature flow. *IMA J. Numer. Anal.*, 35:1622–1651, 2015.

- [21] X. Feng, Y. Li, and Y. Xing. Analysis of mixed interior penalty discontinuous Galerkin methods for the Cahn-Hilliard equation and the Hele-Shaw flow. *SIAM J. Numer. Anal.*, 54(2):825–847, 2016.
- [22] X. Feng and A. Prohl. Error analysis of a mixed finite element method for the Cahn-Hilliard equation. *Numer. Math.*, 99:47–84, 2004.
- [23] B. Fornberg. Generation of finite difference formulas on arbitrarily spaced grids. *Math. Comp.*, 51(184):699–706, 1988.
- [24] B. Fornberg. Classroom note: Calculation of weights in finite difference formulas. *SIAM review*, 40(3):685–691, 1998.
- [25] D. Gottlieb and S. A. Orszag. *Numerical analysis of spectral methods: theory and applications*. SIAM, 1983.
- [26] S. Gottlieb and C. Wang. Stability and convergence analysis of fully discrete Fourier collocation spectral method for 3-D viscous Burgers’ equation. *J. Sci. Comput.*, 53:102–128, 2012.
- [27] J. Guo, C. Wang, S.M. Wise, and X. Yue. An H^2 convergence of a second-order convex-splitting, finite difference scheme for the three-dimensional Cahn-Hilliard equation. *Comm. Math. Sci.*, 14:489–515, 2016.
- [28] J. Guo, C. Wang, S.M. Wise, and X. Yue. An improved error analysis for a second-order numerical scheme for the Cahn-Hilliard equation. *J. Comput. Appl. Math.*, 388:113300, 2021.
- [29] Y. Hao, Q. Huang, and C. Wang. A third order BDF energy stable linear scheme for the no-slope-selection thin film model. *Commun. Comput. Phys.*, 29:905–929, 2021.
- [30] J. S. Hesthaven, S. Gottlieb, and D. Gottlieb. *Spectral methods for time-dependent problems*, volume 21. Cambridge University Press, 2007.
- [31] D. Hou and Z. Qiao. An implicit–explicit second-order BDF numerical scheme with variable steps for gradient flows. *J. Sci. Comput.*, 94(2):39, 2023.
- [32] A. Iserles. *A first course in the numerical analysis of differential equations*, volume 44. Cambridge University Press, 2009.
- [33] C. Lee, D. Jeong, J. Shin, Y. Li, and J. Kim. A fourth-order spatial accurate and practically stable compact scheme for the Cahn-Hilliard equation. *Physica A*, 409:17–28, 2014.
- [34] D. Li and Z. Qiao. On second order semi-implicit Fourier spectral methods for 2D Cahn-Hilliard equations. *J. Sci. Comput.*, 70:301–341, 2017.
- [35] W. Li, W. Chen, C. Wang, Y. Yan, and R. He. A second order energy stable linear scheme for a thin film model without slope selection. *J. Sci. Comput.*, 76(3):1905–1937, 2018.
- [36] X. Li, Z. Qiao, and C. Wang. Convergence analysis for a stabilized linear semi-implicit numerical scheme for the nonlocal Cahn-Hilliard equation. *Math. Comp.*, 90:171–188, 2021.
- [37] X. Li, Z. Qiao, and C. Wang. Stabilization parameter analysis of a second order linear numerical scheme for the nonlocal Cahn-Hilliard equation. *IMA J. Numer. Anal.*, 43(2):1089–1114, 2023.

- [38] X. Li, Z. Qiao, and C. Wang. Double stabilizations and convergence analysis of a second-order linear numerical scheme for the nonlocal Cahn-Hilliard equation. *Sci. China Math.*, 67(1):187–210, 2024.
- [39] Y. Li, H. Lee, B. Xia, and J. Kim. A compact fourth-order finite difference scheme for the three-dimensional Cahn-Hilliard equation. *Comput. Phys. Commun.*, 200:108–116, 2016.
- [40] J.-G. Liu and C. Wang. A fourth order numerical method for the primitive equations formulated in mean vorticity. *Commun. Comput. Phys.*, 4:26–55, 2008.
- [41] J.-G. Liu, C. Wang, and H. Johnston. A fourth order scheme for incompressible Boussinesq equations. *J. Sci. Comput.*, 18(2):253–285, 2003.
- [42] X. Meng, Z. Qiao, C. Wang, and Z. Zhang. Artificial regularization parameter analysis for the no-slope-selection epitaxial thin film model. *CSIAM Trans. Appl. Math.*, 1(3):441–462, 2020.
- [43] S.A. Orszag and C.M. Bender. Advanced mathematical methods for scientists and engineers. *Mac Graw Hill*, 1978.
- [44] Z. Qiao, C. Wang, S.M. Wise, and Z. Zhang. Error analysis of an energy stable finite difference scheme for the epitaxial thin film growth model with slope selection with an improved convergence constant. *Int. J. Numer. Anal. Model.*, 14:283–205, 2017.
- [45] R. Samelson, R. Temam, C. Wang, and S. Wang. A fourth-order numerical method for the planetary geostrophic equations with inviscid geostrophic balance. *Numer. Math.*, 107(4):669–705, 2007.
- [46] H. Song. Energy stable and large time-stepping methods for the Cahn-Hilliard equation. *Inter. J. Comput. Math.*, 92:2091–2108, 2015.
- [47] E. Tadmor. The exponential accuracy of Fourier and Chebyshev differencing methods. *SIAM J. Numer. Anal.*, 23:1–10, 1986.
- [48] C. Wang, J.-G. Liu, and H. Johnston. Analysis of a fourth order finite difference method for the incompressible Boussinesq equations. *Numer. Math.*, 97(3):555–594, 2004.
- [49] Z. Xia, C. Wang, L. Xu, and Z. Zhang. A third order accurate in time, fourth order finite difference scheme for the harmonic mapping flow. *J. Comput. Appl. Math.*, 401:113766, 2022.
- [50] Y. Yan, W. Chen, C. Wang, and S.M. Wise. A second-order energy stable BDF numerical scheme for the Cahn-Hilliard equation. *Commun. Comput. Phys.*, 23:572–602, 2018.
- [51] M. Yuan, W. Chen, C. Wang, S.M. Wise, and Z. Zhang. A second order accurate in time, energy stable finite element scheme for the Flory-Huggins-Cahn-Hilliard equation. *Adv. Appl. Math. Mech.*, 14(6):1477–1508, 2022.